

**COMMUNITY DYNAMICS OF ARCHAEA IN AN ESTUARINE RIVER WATER  
COLUMN AND IMPLICATIONS FOR ARCHAEOLOGICAL BIOGEOCHEMISTRY**

by  
Justin Guider

A thesis submitted to the Faculty of the University of Delaware in partial  
fulfillment of the requirements for the degree of Master of Science in Marine Studies

Summer 2022

© 2022 Justin Guider

All Rights Reserved

**COMMUNITY DYNAMICS OF ARCHAEA IN AN ESTUARINE RIVER WATER  
COLUMN AND IMPLICATIONS FOR ARCHAEOAL BIOGEOCHEMISTRY**

by  
Justin Guider

Approved: \_\_\_\_\_  
Sunita R. Shah Walter, Ph.D.  
Professor in charge of thesis on behalf of the Advisory Committee

Approved: \_\_\_\_\_  
Mark Moline, Ph.D.  
Director of the School of Marine Science and Policy

Approved: \_\_\_\_\_  
Fabrice Veron, Ph.D.  
Interim Dean of the College of Earth, Ocean, and Environment

Approved: \_\_\_\_\_  
Louis F. Rossi, Ph.D.  
Vice Provost for Graduate and Professional Education and  
Dean of the Graduate College

## ACKNOWLEDGEMENTS

I would like to express my sincere gratitude to all those who have supported me both academically and personally throughout my time at the University of Delaware, without whom this work would not have been possible. I am grateful to my advisor Sunita Shah Walter for her constant counsel, support and patience. Many thanks are owed to my committee members Yu-Ping Chin and Jennifer Biddle for their wise advice. I would also like to extend a particular thank you to Dr. Biddle for graciously allowing me to use her lab and office space.

My project would not have been possible without help from myriad members of Dr. Biddle's lab both past and present, including Christina Baughan, Malique Bowen, Sabrina Beckman, Ibrahim Farag, and Kristin Yoshimura. These individuals were my guides through the world of microbial ecology and their assistance was indispensable. Additionally, I would like to thank the following former and current lab mates who helped me with the sampling and sample processing for my project: Alina Ebling, Alexander Rubin, Matthew Hicks, Ethan Goulart, and Leland Wood. Their help with my project as well as their friendship and conversation was greatly appreciated.

I owe a debt of gratitude to the University of Delaware for providing the funding for my research, first through the Marian R. Okie Fellowship and then through a University of Delaware Research Foundation grant. Gratitude is also owed to the donors who support the Marian R. Okie Fellowship. Furthermore, data processing for this project was made possible through use of the University of Delaware CBCB Bioinformatics Core

Facility's BIOMIX computer cluster, funded by Delaware INBRE (NIH NIGMS P20 GM103446), the State of Delaware, and the Delaware Biotechnology Institute.

Finally, I never would have made it this far without the love and support of my parents, Bernadette and Tom Guider, who have believed in me every step of the wa

# TABLE OF CONTENTS

LIST OF TABLES.....	vii
LIST OF FIGURES.....	viii
ABSTRACT.....	x
Chapter	
1. INTRODUCTION.....	1
1.1 Background.....	1
1.2 Study Site.....	2
1.3 Abundant Marine Archaea.....	3
1.4 Time Series and Phenology.....	6
1.5 Estuaries and Their Planktic Archaea.....	9
1.6 Hypotheses.....	13
2. METHODS.....	15
2.1 Sampling.....	15
2.2 Sample Processing.....	16
2.3 Chemical Analyses.....	17
2.3.1 Physical and Chemical Parameters Measured by Sensors.....	17
2.3.2 Nitrate and Nitrite Analyses.....	18
2.3.3 Chlorophyll Analysis.....	18
2.3.4 Other Analyses.....	19
2.4 DNA Extraction and Sequencing.....	20
2.4.1 DNA Extraction.....	20
2.4.2 PCR and Gel Electrophoresis.....	20
2.4.3 Sequencing and Bioinformatics.....	22
2.5 Lipid Extraction.....	25
3. RESULTS.....	27
3.1 Physical and Chemical Parameters.....	27
3.2 DNA Yield.....	28
3.3 Relative Abundance of Classes.....	29
3.4 Alpha Diversity.....	31
3.5 Indicator Species Analysis.....	32
3.6 Explanatory Variables.....	32

4. DISCUSSION.....	36
4.1 Factors Explaining Community Structure.....	37
4.2 Nitrososphaeria (MGI).....	40
4.3 Thermoplasmata (MGII).....	42
4.4 Methanogen Classes.....	46
4.5 Other Anaerobic Classes.....	51
4.6 Unclassified Taxa.....	52
 CONCLUSION.....	 55
 FIGURES AND TABLES.....	 56
 REFERENCES.....	 71
 Appendix	
A SUPPLEMENTAL FIGURES.....	92
B SUPPLEMENTAL TABLES.....	102

## LIST OF TABLES

Table 1:	Sampling dates and corresponding data from YSI Prosolo probe.....	66
Table 2:	Results of linear regressions of MGI, MGII, and methanogen relative abundance vs. environmental variables and Wilcoxon signed rank test...67	67
Table 3:	Results of Indicator Species Analysis test.....	68
Table 4:	Results of ANOSIM test (all samples).....	69
Table 5:	Results of Mantel test (all samples).....	70
Table B.1:	Nucleotide sequences and references for primers used.....	101
Table B.2:	Sampling dates and corresponding ancillary water chemistry data.....	102
Table B.3:	Results of linear regressions comparing relative abundance of methanogens vs. MGI and MGII, relative abundance of Methanobacteria vs. Methanocellia, and the sum of the relative abundance of the four major methanogen classes vs. temperature.....	103
Table B.4:	Results of ANOSIM test (separated by pore size).....	104
Table B.5:	Results of Mantel test (separated by pore size).....	105

## LIST OF FIGURES

Figure 1:	Time series of environmental data.....	56
Figure 2:	Rarefaction curves after removing low-abundance OTUs.....	57
Figure 3:	Community composition of archaea from the largest pore size.....	58
Figure 4:	Community composition of archaea from the middle pore size.....	59
Figure 5:	Community composition of archaea from the smallest pore size.....	60
Figure 6:	Scatterplot and box plot of DNA concentrations from each filter type....	61
Figure 7:	Abundance of MGI, MGII and methanogens over time.....	62
Figure 8:	Box plots of alpha diversity comparing samples grouped by category....	63
Figure 9:	NMDS plot of all samples with colors denoting categorical variables.....	64
Figure 10:	NMDS plot of all samples coded by filter type and time of year with pseudo-axes.....	65
Figure A.1:	Location of the study site and sampling setup.....	92
Figure A.2:	Plots of ancillary data over time.....	93
Figure A.3:	Annotated example of a successful gel.....	94
Figure A.4:	Rarefaction curves before removing low-abundance OTUs.....	95
Figure A.5:	Box plot of monthly chlorophyll a concentrations and total nitrogen in the Broadkill river from 2001-2022.....	96
Figure A.6:	Stress plot for ordination of Bray-Curtis dissimilarity.....	97
Figure A.7:	NMDS plots created from separate ordinations for each pore size with colors denoting categorical variables.....	98
Figure A.8:	NMDS plots created from separate ordinations for each pore size with pseudo-axes.....	99

Figure A.9: Box plots of alpha diversity comparing samples grouped by category;  
separated by pore size.....100

## ABSTRACT

In the past three decades, it has been established that archaea play important biogeochemical roles in the marine water column and sediments, but there remains a gap in knowledge about the phenology of these marine planktic archaea. Even less is known about their phenology and diversity in estuarine environments than in marine environments. Here I report the results of a year-long census of archaeal diversity created by filtering water from the Broadkill River, an estuarine river mouth in Delaware, USA, and sequencing the DNA extracted from filters. These results provide information on how the archaeal community, at the class level, changed over time, as well as based on particulate size fraction, tides, and environmental parameters such as temperature and salinity. The most important factor affecting community composition was particle size, suggesting a partitioning of archaea into particle-associated and free-living groups. Seasonal and tide-based trends, while not important in explaining overall diversity, were evident for several classes of archaea. Of particular interest were Nitrososphaeria (Marine Group I), the relative abundance of which correlated with tide, and Thermoplasmata (Marine Group II), which increased in relative abundance during the warmer months. The dominance of the community by Thermoplasmata during the summer presents an opportunity to investigate this uncultured group's membrane lipids in the future. Methanogens and other anaerobic archaea were present in greater abundance in the larger size fraction, suggesting the use of anoxic particle interiors and active anaerobic metabolism in the water column.

## Chapter 1

### INTRODUCTION

#### 1.1 Background

Numerous studies have investigated the phenology of marine bacterioplankton in the surface ocean and found consistent seasonal trends in the abundance of both common and rare taxa (Fuhrman et al. 2006, Gilbert et al. 2011). However, due in part to their recent discovery, considerably less is known about how marine planktic archaea vary in abundance over time (DeLong 1992). The research that has been done on marine archaeal community composition has focused on environments such as the Black Sea (Sollai et al. 2019), polar ocean (Church et al. 2003), and open ocean (Baltar et al. 2007), but comparatively few studies have examined the diversity and phenology of planktic archaea in estuaries. Bacterial community structure can change drastically along a salinity gradient (Campbell and Kirchman 2013), and the same is likely true of archaeal communities. Estuaries are unique environments in that they exist at the conflux of fresh and saltwater, and this leads to a unique mixed community of freshwater and saltwater microbes (Crump et al. 1999). Indeed, the few studies comparing archaeal diversity between estuarine and pelagic environments have found significant differences between the two (Anas et al. 2021, Tee et al. 2021). Some research has focused only on particular functional groups or taxa, for example ammonia oxidizers (Francis et al. 2005, Santoro and Casciotti 2011) and methanogens (Levipan et al. 2007), rather than the community as a whole. Furthermore, while it is clear that planktonic community structure can change

dramatically in a short period of time (Guadayol et al. 2009), few studies have sampled a single location over time to characterize temporal changes. Those that have, have done so in non-estuarine environments (e.g., Galand et al. 2010, Hugoni et al. 2013). A reoccurring census of the entire archaeal community in a coastal estuary is a missing puzzle piece in our understanding of marine microbial community dynamics. Given the importance of marine planktonic archaea in biogeochemical cycling (Offre et al. 2013), understanding how the marine planktic archaeal community changes over time would improve our understanding of the ecology of estuaries as a whole.

## **1.2 Study Site**

The Broadkill River is a tidal river located in Sussex County, Delaware. It delivers riverine and land-derived material and biomass to the Delaware Bay via the Roosevelt Inlet. This study's sampling site was located on the University of Delaware's Hugh R. Sharp campus in Lewes, Delaware, approximately 250 meters from the Roosevelt Inlet. At this terminal end of the river, the water column is well mixed; in fact, it is completely vertically homogeneous in terms of physical and chemical parameters for 90% of the tidal cycle. This is the result of the strong tidal currents at work, which lead to water from the Bay passing through the river channel which, at its mouth, is only about 4 meters deep and 100 meters across (Dewitt and Daiber, 1973). This results in very little vertical stratification of salinity and temperature. At high tide, the temperature, salinity, pH, dissolved oxygen concentration, and total dissolved solids of the river mouth are similar to those of the lower Delaware Bay; at low tide, they are similar to those of the upper river (Dewitt and Daiber 1973). This tidally-driven contrast in conditions at the

Broadkill River mouth presents the opportunity to compare river and marine influences at this single site. The Broadkill River has more suspended particles at upriver sites (Dewitt and Daiber 1973, Yoshimura et al. 2018) and has no annual trend in chlorophyll a concentrations or total nitrogen (DNREC et al. 2022).

### **1.3 Abundant Marine Archaea**

Globally, the two most abundant archaeal taxa in the marine water column are Marine Group I (MGI) and Marine Group II (MGII) (Hugoni et al. 2013, DeLong 2021, Santoro et al. 2019). MGI have a cultivated representative, *Nitrosopumilus maritimus*, and thanks to this, more is known about their physiology and metabolism than any other planktic marine archaea (Könneke et al. 2005). They are chemoautotrophs that gain the energy to reduce bicarbonate into organic carbon by oxidizing ammonia to nitrite (Walker et al. 2010, Pester et al. 2011). There is evidence that some may be mixotrophic (Ingalls et al. 2006, Ouverney and Fuhrman 2000, Teira et al. 2006), but autotrophic ammonia oxidation is the dominant metabolic strategy. In fact, they are the dominant ammonia oxidizers in the marine water column (Wuchter et al. 2006), outcompeting bacteria thanks to their tolerance for low-oxygen concentrations and more efficient carbon fixation pathway (Pester et al. 2011, Könneke et al. 2014). Understanding the major role that MGI play in the marine nitrogen cycle has initiated a paradigm shift from a few decades ago where archaea were thought to play no significant role in the biogeochemistry of the marine water column. This raises the question: what ecological role do other planktic archaea play in the surface ocean? There are no cultured representatives of the abundant but variable MGII, but thanks to metagenome-assembled

genomes and culture experiments we know that they are likely heterotrophs that degrade high-molecular weight organic compounds such as those produced by marine diatoms (Iverson et al. 2012, Orsi et al. 2015). Most also contain the gene for proteorhodopsin, and the greater prevalence of this gene among MGII in surface waters suggest they use sunlight to create extra energy (Frigaard et al. 2006, Rinke et al. 2019). Other archaeal taxa (e.g. Bathyarchaeota, Halobacteria, and various methanogens) show up frequently in estuarine water column environments but are typically not detected in the open ocean. Many of these groups are typically associated with sediment and their biogeochemical and numerical importance in the water column is uncertain (Sollai et al. 2018; Biddle et al. 2006).

A topic of great interest to scientists who study marine archaea is their membrane lipids, which are easily distinguished from bacterial membrane lipids. As a result, much effort has been made to identify particular lipids as biomarkers for archaeal taxa (Sturt et al. 2004, Wakeham et al 2004). The cultivation of *N. maritimus* has revealed the membrane lipids of MGI archaea, but the distribution of lipids produced by uncultured archaea such as MGII is as of yet unclear. Crenarchaeol, a glycerol biphytanyl glycerol tetraether (GDGT) lipid, is widely considered to be produced only by MGI archaea and other members of the phylum Thaumarchaeota (formerly within Crenarchaeota) (Brochier-Armanet et al. 2008, Pester et al. 2011). However, there has been much debate over whether MGII might also produce crenarchaeol and other GDGTs believed by many to be unique to MGI and related archaea (Lincoln et al. 2014a, Lincoln et al. 2014b, Schouten et al. 2014, Turich et al. 2007, Schouten et al. 2008, Turich et al. 2008), with

recent studies continuing to report conflicting results (Besseling et al. 2020, Ma et al. 2020). Understanding which groups produce which lipids is important not just for evaluating the viability of using lipids as biomarkers but because a proxy for past sea surface temperatures, TEX86, relies upon the relative abundance of GDGTs in sediment (Schouten et al. 2002). The identification of a site even temporarily dominated by MGII would present the opportunity to gain insight into the group's membrane lipids.

A note about taxonomy: taxonomic designations for MGI and MGII have changed over the years. MGI was originally placed in the phylum Crenarchaeota, subsequently moved to its own phylum, Thaumarchaeota, and now is placed in the phylum Thermoproteota and class Nitrososphaeria. MGII, once classified in the phylum Euryarchaeota, is now classified as phylum Thermoplasmata and class Poseidoniia (Brochier-Armanet et al. 2008, Parks et al. 2020, Rinke et al. 2020). However, the Silva database (v138\_1) (Quast et al. 2013) used to classify sequences for this study locates MGI/Nitrososphaeria in the phylum Thaumarchaeota and MGII in the class Thermoplasmata. The analyses in this paper considers primarily the class-level distinctions due to limitations in the resolution of sequence data and, for simplicity's sake, the classes Nitrososphaeria and Thermoplasmata will be used interchangeably with MGI and MGII. These taxa contain orders other than MGI and MGII, but MGI and MGII are the dominant member of those classes in the marine water column (Rinke et al. 2019, Santoro et al. 2019) including at the study site sampled for this project (Yoshimura et al. 2018).

## 1.4 Time Series and Phenology

Several studies have investigated archaeal community structure over a time series in the marine water column. One purpose of time series studies is to investigate seasonal trends in the abundance of key taxa. Such studies can provide information about the ecology of these taxa when paired with measurements of biotic (e.g. chlorophyll concentration, abundance of bacteria and eukaryotes) and abiotic (e.g. salinity, temperature, nutrient concentrations) factors (Galand et al. 2010, Liu et al. 2018). There are numerous studies that investigate archaeal populations in pelagic settings compared to a more limited number in coastal settings. Generally, pelagic water column studies have focused on the most abundant groups, MGI and MGII, even using specific oligonucleotide probes to target them at the exclusion of other taxa (Quiñones et al. 2009, Beman et al. 2011, Molina et al. 2020). This is reasonable for pelagic studies given that MGI and MGII are by far the most abundant archaeal groups in the epipelagic ocean (Santoro et al. 2010). The abundance of both MGI and MGII changes throughout the year, but bloom events are more common for MGII. Blooms can appear sporadic, following no apparent seasonal trend in some locations and regularly occurring in other locations. Beman et al. (2011) studied a 4-year long time series in coastal California waters and saw peaks in abundance for both MGI and MGII, but these did not follow seasonal trends; instead, they identified several groups of bacteria whose abundance was correlated with that of MGI and/or MGII. Quiñones et al. (2009) likewise did not identify any seasonal trends in MGI or MGII abundance in their time series study of archaea in the Humboldt current.

In the shallow ocean, Marine Group I is often found in higher abundance in the winter (Wuchter 2006, Galand et al. 2010, Herfort et al. 2007, Hugoni et al. 2013), although at least one study found it to be more abundant in summer and fall than in winter and spring (Molina et al. 2020). MGI archaea are autotrophic or mixotrophic, obtaining their energy from oxidation of ammonium to nitrite or a combination of ammonia oxidation and heterotrophy (Walker et al. 2010, Ingalls et al. 2006). It is not surprising, therefore, that their abundance is often found to correlate with the abundance of the *amoA* gene, which encodes a subunit of the ammonia monooxygenase enzyme (Herfort et al. 2007, Galand et al. 2010), as well as with the concentration of nitrogen compounds (Herfort et al. 2007, Hugoni et al. 2013), nitrite in particular (Smith et al., 2015; Hurley et al., 2018); they are not found to bloom during algal blooms. More enigmatic is the ecology of Marine Group II, whose abundance is not typically correlated with nutrient abundance (Murray et al. 1999). Given the expected use of phytoplankton-derived organic carbon by MGII, many studies have examined MGII abundance in the context of phytoplankton abundance, often using chlorophyll concentration as a proxy. MGII blooms often occur in spring and summer, times of high phytoplankton productivity in many regions (Pernthaler et al. 2002, Wuchter 2006, Herfort et al. 2007, Needham and Furhman 2016). Murray et al. (1999) found that MGII abundance did not covary with chlorophyll a concentrations in the Santa Barbara Channel over a multi-year timeseries, but some MGII blooms followed chlorophyll peaks. In the North Sea, Wuchter (2006) connected MGII blooms to phytoplankton blooms in a time series study of planktic archaea abundance measured by qPCR and CARD-FISH and Herfort et al.

(2007) identified a spatial as well as temporal correlation of MGII relative abundance (measured by qPCR) with chlorophyll a concentration. Needham and Fuhrman (2016), in their study of MGII abundance measured by PCR off the coast of southern California, identified a MGII bloom immediately following a phytoplankton bloom. These bloom events of MGII can be quite significant. MGII can represent greater than 30% of the total prokaryotic community during blooms, much higher than their typical abundance (Needham and Fuhrman 2016, Pernthaler et al. 2002, Orellana et al. 2019).

One factor that might complicate our understanding of MGII phenology is the presence of multiple phylotypes that occupy different niches. Two time-series studies conducted in the Mediterranean Sea identified two primary ecotypes of MGII: MGIIa and MGIIb. MGIIa bloomed in summer, MGIIb in winter (Galand et al. 2010, Hugoni et al. 2013). These studies also identified a potential link between MGII abundance and chlorophyll concentration, but only for MGII.b. Galand et al. (2010) attributed the MGII.a peak in winter to summer stratification of the Mediterranean water column. Orellana et al. (2019) also identified these two phylotypes, and also reported higher abundance of MGII.a in summer and MGII.b in winter. The authors connected the reoccurring MGII.a blooms to phytoplankton blooms, and hypothesized that the small cell size of this phylotype may help them avoid grazing and so benefit from blooms. From all of these studies, a connection between phytoplankton blooms and MGII abundance seems likely, but the dynamics differ in different systems: sometimes there is a lag between phytoplankton blooms and MGII blooms, and sometimes there is none; other factors such as stratification of the water column may influence the timing and

magnitude of MGII blooms; and the different niches occupied by different phylotypes may obscure relationships if one considers MGII as a whole.

### **1.5 Estuaries and their Planktic Archaea**

It is clear from these studies that the community dynamics of even pelagic systems can be quite different from each other; the dynamics are likely quite different in an estuarine system, but no comparable time-series study of archaeal community dynamics in an estuary exists. Furthermore, diversity tends to be higher in estuaries, with groups other than MGI and MGII often making up large proportions of the community (Liu et al. 2018). The few papers that have reported archaeal diversity of estuaries have yielded an intriguing array of results. Yoshimura et al. (2018) sequenced archaeal 16S rRNA genes taken from a transect of sites in the Broadkill River with a particular focus on the differences between upriver/downriver sites and between particle-associated and free-living microbes. They found that upriver stations were dominated by Halobacteria in the free-living fraction and Halobacteria and Methanomicrobia in the particle-associated fraction. Their “marine” station, the same station that was sampled for this project, was dominated by Thermoplasmata, the vast majority of which could be further classified as Marine Group II (MGII). This finding was a major impetus for this thesis work. However, as valuable as this study’s findings were, sampling of the “marine” station took place at a single date in July, and so only captured a snapshot of the community at that time. Anas et al. (2021) sampled a transect from the Coochin Estuary in India to the Arabian Sea. They found that their estuarine site was more diverse than their more marine sites, but most of their Operational Taxonomic Units (OTUs), analogous to

species, could not be classified at all. What could be classified was mostly Nitrosopumilaceae in the class Nitrososphaeria. Thermoplasmata was also observed but never in high abundance. As with Yoshimura et al. (2018), their sampling took place at a single date, in this case in August. An additional study examined archaeal diversity along a river-to-estuary transect in New Zealand, also at one date (November) at low tide (Tee et al. 2021). This study found an archaeal community composed of Bathyarchaea, Methanocellales, Methanomicrobiales, Woesearchaeales (class Nanoarchaeia), and MGI (class Nitrososphaeria).

The most comprehensive study of archaeal diversity in estuaries comes from Liu et al. (2018), who used as their dataset 16S rRNA genes uploaded to a database, representing 24 estuaries worldwide. They found that the most abundant archaeal phyla in estuarine water columns worldwide were Thaumarchaeota (containing Nitrososphaeria/MGI); Bathyarchaeota; and Euryarchaeota (at the time containing Thermoplasmata/MGII). They also found a trend in the abundance of many groups based on latitude and environmental factors. Thermoplasmata was more abundant in low and high latitudes and its abundance was influenced by temperature. MGII was more abundant in low latitudes. The authors noted that certain OTUs were present across many estuaries while others were far more localized. This highlights the importance of understanding local dynamics; every estuary is unique. The authors also noted the presence of OTUs that could not be confidently identified by current databases, suggesting the potential for the discovery of novel archaeal taxa in estuaries. This potential for the discovery of novel estuarine taxa was also noted by Vieira et al. (2007)

in their study of archaea in a tropical estuary in Brazil. Given the limitations of their methodology, however, Liu et al. (2018) were unable to determine relationships between archaeal diversity and tides or seasonality within any given estuary.

High turbidity distinguishes estuaries from the open ocean due to high loads of suspended particulate matter (Shi and Wang 2010). This has implications for the structure of the microbial community of the estuarine vs. the open ocean water column, since sediment particles can become entrained in the water (Crump et al. 1999). Microbes are known for taking advantage of microhabitats, including the distinct conditions found on the exterior vs. interior of particles. In estuaries, more than half of the bacterioplankton present can be associated with particles, and more than 90% of the bacterial carbon production in these systems can be attributed to particle-attached bacteria. Studies of marine and estuarine archaeal communities have found a divide between free-living and particle-associated groups (Kellogg and Deming 2009, Yoshimura et al. 2018, Vieira et al. 2007). Particle-attached microbial populations can also be responsible for a large proportion of the organic matter degradation occurring in estuaries (Crump et al. 1998, Crump and Baross 1996). The shallow depth of estuaries compared to the open ocean also contributes to sediment resuspension (Crump and Baross 1996). This mechanism connects populations of water column and sediment microbes. Particles may deliver their associated microbes from water column to sediment (Mestre et al. 2018), and it is conceivable that microbes on particles suspended from sediment may continue their metabolic activities and thus influence biogeochemical cycling in the water column.

Particle interiors can offer an anoxic or hypoxic environment within an oxygenated water column, allowing for oxygen-inhibited metabolic processes such as methanogenesis that would otherwise be thermodynamically unfavorable in an oxic water column (Simon et al. 2002). Methanogenic archaea (and indeed all methanogens are archaea (Offre et al. 2013, Lyu et al. 2018)) such as *Methanosarcina* and *Methanomicrobia* have been found to be associated with anoxic particle interiors in estuaries (Smith et al. 2013). Methanogenesis occurs in oxic regions of freshwater (Bogard et al. 2014) and marine (Damm et al. 2010, Leonte et al. 2020) ecosystems. Bogard et al. (2014) found that 4% of all greenhouse gas contribution from a freshwater lake was from methanogenesis occurring in the oxic water column, and that this number could be higher in systems with higher productivity and deeper water columns. Leonte et al. (2020) found methane production in the aerobic water column to be a more important source of methane than seafloor gas seeps, although they also determined that methane concentrations are kept low by active aerobic methanotrophy. Methanogens are sometimes detected in studies of archaeal diversity in estuarine water columns and sometimes not. Tee et al. (2021), Anas et al. (2021), Yoshimura et al. (2021), and Vieria et al. (2007) all reported the presence of methanogens in the water column; Liu et al. (2018), and Hao et al. (2010) did not. Interestingly, one study from the Pearl River Estuary in China did not report the detection of methanogens (Liu et al. 2014), whereas another found them in great abundance, making up most of the community at upriver sites (Chen et al. 2019). This diversity of findings raises the questions of how important

these water column-dwelling methanogens are to global organic carbon degradation and what factors determine their presence or absence.

## **1.6 Hypotheses**

The time series of estuarine archaeal community composition and environmental parameters presented in this thesis represents a unique set of data that will help shed light on the factors that drive changes in archaeal diversity and the abundance of individual archaeal classes over time. The experimental design allows me to investigate these questions with a focus on the archaeal community as a whole as well as resolve differences between discrete size classes of particles.

I hypothesized that seasonality and the factors that change with the seasons, namely temperature and light availability (PAR), would exert a strong influence on the composition of the archaeal community and would drive changes in the abundance of individual archaeal classes from season to season. I expected the influence of season to be particularly pronounced for MGII and predicted that this group would experience a bloom in the summer. I further hypothesized that tidal stage, and salinity by proxy, would also be a strong control on archaeal community composition. High tide and high salinity would represent a greater marine influence from the Delaware Bay while low tide and low salinity conditions would correspond with a greater influence from the Broadkill River. I expected archaeal communities at high tide to more closely resemble a pelagic water column community with low diversity and a dominance of MGI and MGII archaea. At low tide, I hypothesized greater similarity with riverine and estuarine communities,

higher diversity and a greater presence of anaerobic archaeal taxa such as methanogens, Halobacteria, Bathyarchaea and Nanoarchaea, with MGI and MGII still present.

In addition to seasons and tides, I hypothesized that I would see a relationship between MGII abundance and peaks in the concentration of total chlorophyll and DOC concentration due to an association between MGII and phytoplankton blooms. I expected to see a relationship between MGI and nitrate, nitrite or total nitrogen, but did not expect this for MGII. Finally, I expected to see higher diversity in particles captured on large pore size filters (particle-associated archaea) vs. smaller particles or free-living archaea captured on the smallest pore size filters as the larger particles would likely accommodate microhabitats with conditions supporting anaerobes.

The original objective of this project was to couple the investigation of the archaeal community using 16S rRNA gene sequencing to the lipids present using HPLC/MS. Technical challenges prevented the inclusion of lipid data in this work. However, the sequence data presented here open up the possibility for targeted future work investigating MGII lipids in the season and particle size where they are dominant.

## Chapter 2

### METHODS

#### 2.1 Sampling

Monthly water samples for this project were taken near the mouth of the Broadkill River where it empties into the Delaware Bay via Roosevelt Inlet. Sampling was done from the dock near the Pollution Ecology Lab at the University of Delaware's Hugh R. Sharp campus in Lewes, Delaware (38.790419°N, 75.163378°W) (Figure A.1). The primary objective of sampling was to obtain water from the surface (0 meters) and 1 meter depth in order to capture particulate matter and microbial cells by filtration. A 5-liter General Oceanics Niskin bottle was lowered from a davit on the dock repeatedly to collect 15-20 L of water, which was transferred to acid washed HDPE carboys. Sampling was performed every month for 12 months, from July of 2020 to June of 2021. For the first five months (July through November 2020), sampling was performed once per month; subsequently, sampling was performed twice per month, once during a high slack tide and once during a low slack tide within 8 days of each other. Overall, 11 high tides and 9 low tides were sampled (Table 1).

Ancillary data (Figure 1) was taken at each sampling event. A PNF-300 Profiling Natural Fluorometer System (Biospherical Instruments Inc.) was lowered off the davit to measure the photosynthetically active radiation (PAR) at both depths. The accompanying software LoggerLight was used to collect real-time data from the instrument. A YSI ProSolo ODO/CT probe (YSI Incorporated, Yellow Springs, Ohio) was used to collect

data on chemical and physical water parameters at both depths. To allow for later measurement of dissolved inorganic carbon (DIC), combusted glass bottles were filled with water from the outlet on the Niskin bottle.

## **2.2 Sample Processing**

Sample processing began within 1 hour of sampling. The carboys containing the sample water were returned to lab and placed on ice. DIC bottles were preserved immediately; 20  $\mu$ l of saturated mercuric chloride ( $\text{HgCl}_2$ ) 6.5% solution (LabChem lot # J339-08) were added to each bottle to kill all organisms and so stop respiration and photosynthesis. To minimize gas exchange, Apiezon M grease was applied to the inside of the ground glass joint of BOD bottles and the bottle was sealed with a stopper and further secured with a rubber band. If using a bottle with a threaded cap, the cap was very tightly sealed and Parafilm was wrapped around the cap to help mitigate gas exchange with the bottle's contents. DIC samples were stored in a dark drawer until they were processed.

Filtration of the collected water was necessary to concentrate particulate material and microbial cells for later lipid extraction, DNA extraction, and chlorophyll analysis. The water from each carboy was filtered using a peristaltic pump and acid-washed Masterflex BioPharm tubing. Sample water was passed through a series of three in-line Advantec polypropylene 47mm filters holders with pre-combusted glass fiber filters (450°C for 1 hour and 500°C for 2 hours) of decreasing pore size: Whatman GF/D (nominal pore size 2.7  $\mu$ m), Whatman GF/F (nominal pore size 0.7  $\mu$ m), and Advantec GF-75 (nominal pore

size 0.3  $\mu\text{m}$ ). The exception was that for the first one or two sets of filters, a 0.22  $\mu\text{m}$  Millipore GSWP nitrocellulose filter replaced the GF-75, and these were later used for DNA extraction. Water was filtered until the flow rate through the distal end of the tubing slackened and the tubing began to shake, indicating the build-up of backpressure due to a clogged GF/D filter. At this point the filtration was paused and each filter was folded into a pre-combusted foil packet which was immediately transferred to a  $-80^{\circ}\text{C}$  freezer. The forceps used to transfer the filters were solvent-rinsed between each set. The filters were replaced and filtering resumed; this was repeated until 4 – 17 (average 9.4) liters of water had been passed through all sets of filters for each carbo-. During this process, 40 ml of filtered water was collected for both depths and stored in EPA vials in a  $-20^{\circ}\text{C}$  freezer for later nitrate/nitrite and DOC analysis.

## **2.3 Chemical analyses**

### **2.3.1 Physical and Chemical Parameters Measured by Sensors**

A YSI ProSolo probe was used to measure water temperature, salinity, dissolved oxygen, and total dissolved solids. The instrument probe was lowered into the water by the cord; to get surface measurements, it was lowered until all sensors were submerged. The cord was marked at 1 m so that the probe could be lowered to that depth as well. After submerging, the probe was given a shake to dislodge any internal air bubbles. Data were recorded on the instrument once readings stabilized. The dissolved oxygen sensor was calibrated approximately every other month by exposure to water-saturated air. The salinity sensor was calibrated at the same time using a conductivity standard (YSI 3168

Conductivity Calibrator). Data were uploaded from the instrument to the YSI software KorDSS.

### **2.3.2 Nitrate and Nitrite Analyses**

Nitrate and nitrite (Figure A.2) were measured by UV-Vis spectrophotometry on a HP Diode Array Spectrophotometer paired with the software Olis Globalworks. Frozen filtered water samples were thawed then aliquoted into acid-washed plastic vials. To determine nitrite concentrations, aliquots were spiked with Griess reagent and color allowed to develop for 25 minutes before quantification of absorbance. To determine nitrate concentrations, Griess reagent and vanadium chloride in hydrochloric acid were added and samples were heated at 60°C in a water bath for 25 minutes so that all nitrate was reduced to nitrite. Standards (made with  $\text{NaNO}_2$  and  $\text{KNO}_3$ ) were diluted and used to make a standard curve by which concentrations were determined from absorbance values. Nitrate concentration was calculated by subtracting the nitrite concentration of the aliquots that had not been spiked with the reducing agent from those that had nitrate reduced to nitrite by the reducing agent.

### **2.3.3 Chlorophyll Analysis**

Chlorophyll was measured by extracting chlorophyll from a set of paired GF/D and GF/F filters from each sampling date and depth. The filters were left to extract in 10 mL acetone in the -20 freezer for 24 hours, then the supernatant was transferred to a clean pre-combusted 20 mL vial. Samples were kept in the dark as much as possible. Total chlorophyll was quantified on a Turner fluorometer with an excitation filter at 340-500

nm and emission filter at 665 nm. Briefly, 2-5 ml of sample was centrifuged to remove debris, then diluted with 2-3 ml of MilliQ water, depending on concentration. The instrument was warmed up for 20 minutes, a solid standard (Turner secondary standard for chlorophyll) measured, then the samples measured. Data were normalized by dividing total micrograms chlorophyll by the number of L filtered by each filter pair.

#### **2.3.4 Other Analyses**

DIC (Figure A.2) was measured on a Model AS-C5 DIC analyzer (Apollo SciTech). Briefly, intake tubes were purged with 3%  $\text{H}_3\text{PO}_4$  in 7% NaCl then placed in standard and sample bottles.  $\text{N}_2$  flow rate was set to 200 mL/min and a leak test was performed. The instrument was instructed to measure DIC in the standard and each sample via the associated ASC5 X12 software. A Li-Cor infrared gas analyzer was used to quantify the DIC as  $\text{CO}_2$ .

DOC (Figure A.2) was quantified on a Shimadzu TOC-V analyzer linked to the software TOC-Control V. Prior to a run, the instrument was instructed via the software to create a calibration curve using a 10 mM organic carbon standard of potassium hydrogen phthalate. Sample vials, blanks, and check standards were then loaded into the instrument's autosampler. Samples were sparged with acid to remove all DIC. Remaining DOC was oxidized to  $\text{CO}_2$  with a catalyst at 680°C and quantified by an IR detector (Sharp 2002).

## **2.4 DNA Extraction and Sequencing**

### **2.4.1 DNA Extraction**

DNA was extracted from all three filter sizes (GF/D, GF/F, and nitrocellulose) for every sample date and depth. The filters were cut in half or, in the case of the highly-loaded GF/D filters, in thirds; a portion was used for the extraction and the remainder was returned to the -80 freezer. DNA was extracted using a Qiagen Dneasy PowerSoil kit according to kit protocol with the exception that instead of sediment, the filter was folded up and inserted into the bead beating tube. Steps were taken to avoid contamination, including pre-cleaning surfaces and tools by flame sterilization with ethanol. After the full DNA extraction sequence, the DNA-containing extract was stored in a -20 freezer until the next step.

### **2.4.2 PCR and Gel Electrophoresis**

The goal of this step was to produce amplified DNA with Illumina tags to be sequenced at the Microbial Analysis, Resources, and Services (MARS) facility at the University of Connecticut, Storrs (<https://mars.uconn.edu/>). The PCR primers targeted bacterial and archaeal 16S ribosomal RNA genes in order to investigate the taxonomy of the microbes present. Universal primers B114F and B1275R (Denman and McSweeney 2006) and archaeal primers ARCH915F and ARCH1059R (Seyler et al. 2018) were used and are described in Table B.1. Archaea-specific primers were chosen to more closely investigate the archaeal community as they amplify more archaeal sequences than universal primers do (DeLong 1992). The archaea-specific primers used also included

Illumina “tags”, short sequences appended to the 5’ end of the primer that are required by the Illumina sequencing technology. Various rounds of “check PCR” were performed to make sure that bacteria and archaea were present in all samples; DNA amplified by universal primers were not sequenced. All PCR reactions were done using the HotStarTaq mix (Qiagen) which contains Taq polymerase, dNTPs, and buffer. This was mixed with 2  $\mu$ L of sample DNA, PCR-grade water, and 20  $\mu$ M forward and reverse primer solutions. All PCR prep was done in a PCR hood to avoid contamination. The PCR itself was run on an Eppendorf Mastercycler pro. Conditions for DNA with archaeal primers was as follows: denaturation at 94°C for 45 seconds followed by 35 cycles of annealing at 60°C for 1 minute and extension at 72°C for 1 minute. Conditions for DNA with universal primers were identical except the annealing temperature was 55°C. Following amplification, PCR products were cooled to 4°C by the Mastercycler then collected and stored in a -20°C freezer.

Gel electrophoresis was used to confirm that bacterial and archaeal DNA had been amplified successfully. A TAE buffer was used to make a gel with ethidium bromide as the intercalating agent. The gels made for the check PCR were 1% agarose (w/v). They were run for about 15-20 minutes, or until good separation was reached (Figure A.3). Gels were placed in a Carestream Molecular Imaging System and imaged on top of UV light using a Kodak Gel Logic 112 Imaging System. Images were processed for clarity using the Molecular Imaging Software provided by Carestream.

Two sets of samples were submitted to the MARS facility for sequencing: extracted DNA to be amplified with universal primers targeting the v4 region of the 16S

rRNA gene and PCR products amplified with archaea-specific primers and Illumina tags for two-step library prep and sequencing. The two-step process refers to the addition of unique nucleotide identifiers by an additional round of PCR which precedes sequencing (Lange et al. 2014). PCR products were cleaned up using a Thermo Scientific GeneJet PCR Purification Kit. DNA for both types of sample was quantified using Thermo Scientific NanoDrop LITE: between 58.5 and 200.5 ng/ $\mu$ L of purified PCR product and between 0.3 and 193.8 ng/ $\mu$ L of DNA were sent. Extracted DNA was pipetted into sterile 96 well Eppendorf twin.tec plates and shipped to MARS on dry ice.

### **2.4.3 Sequencing and Bioinformatics**

Sequences were processed using the software program mothur (Schloss et al. 2009). Files were hosted and mothur processes run on the computing cluster BIOMIX at the Delaware Biotechnology Institute (DBI). Reverse reads were determined to be of low quality based on a FastQC Report visualization (Andrews 2010) of base sequence quality and so were discarded; only forward reads were used for analysis. An apparent sequencing error produced a string of adenosine (“A”) reads towards the end of every sequence; the software Geneious 9.1.8 (<http://www.geneious.com>) was used to remove these, leaving sequences in the range of 200-212 base pairs long. These were quality filtered to remove sequences with ambiguous nucleotide reads or more than 8 homopolymers. Mothur was used to align sequences, remove repeats, and find pairwise distance between sequences. Sequences were then clustered into OTUs at 3% dissimilarity and binned. Finally, OTUs were classified using the Silva v138\_1 database (Quast et al. 2013). Rarefaction curves showed that most samples did not converge

toward a horizontal asymptote (Figure A.4). In order to determine whether it would be reasonable to remove low abundance OTUs, all OTUs with less than 10 representative sequences in each sample were searched against sequences in all other samples using the BLAST tool (Wheeler et al. 2006). None of these low abundance OTUs matched sequences in any other samples, so they were removed given that the focus of this project was on abundant groups. Rarefaction curves produced after removing low abundance OTUs showed all samples reaching horizontal asymptotes, indicating that the sequencing depth represented the diversity at the study site well (Figure 2).

Rarefaction curves, stacked bar chart, Nonmetric Multidimensional Scaling (NMDS), and other plots were produced using R. Prior to producing the stacked bar charts (Figures 3-5), the data were normalized for the large variability in the number of sequences returned per sample. Rarefaction to a fixed number of sequences and scaling with ranked sampling (SRS) (Beule and Karlovsky 2020) methods were compared given that McMurdie and Holmes (2014) provide arguments for the statistical inadmissibility of rarefying data. Data were rarefied by taking 7000 sequences from each sample. Rarefied and normalized data were nearly identical. The data shown in figures here were produced with the data normalized using SRS. In general, the sequence quality was too poor to get high-resolution taxonomic information – removing the string of A's resulting from a sequencing error resulted in sequences shorter than normal for Illumina sequencing. The following analyses focus on the level of class which distinguishes between the groups of the most interest: MGI and MGII (Nitrososphaeria and Thermoplasmata, respectively). OTUs that represented less than 5% of the sequences in each sample were combined into

an “Other” category prior to creating stacked bar charts. Empty bars in the bar charts indicate missing data. In the case of the first two sampling dates, on 7/21/20 water was sampled at 0 m only; on 7/30/20, water was sampled at 1 m only. Other missing dates for certain pore sizes/dates were unintentionally left out of the samples sent to MARS, except in the case of 2/17/21 at 0 m in the smallest size fraction (nitrocellulose); that sample was intentionally left out because it represented a small number of sequences and was an outlier compared to the sequencing depth of other samples. NMDS plots were produced based on normalized data prior to grouping low-abundance classes into an “Other” category. The normalized data were transformed into a Bray-Curtis dissimilarity matrix before creating the NMDS plots.

Statistical tests were also performed in R. An ANOSIM test with 9999 permutations was employed for each set of categorical variables to provide a statistical evaluation of patterns revealed by the NMDS plots. To investigate which particular classes were more or less abundant based on the different categorical variables, indicator species analysis was used (De Cáceres et al. 2009). Statistical tests involving relationships between taxon abundance and environmental parameters were done using the relative abundance of taxa. A Mantel test was used to find correlations between the Bray-Curtis distances of the community matrix and Euclidean distance matrices of environmental variables. Alpha diversity was calculated from normalized data. Simpson’s Diversity Index and the Shannon-Wiener Diversity Index were used to calculate Alpha diversity. A Tukey’s Honest Significant Different test based on ANOVA test results was performed to determine whether alpha diversity was different among high vs. low tide, pore size,

depth, and season. A Tukey's test was also used to compare DNA yields from the three types of filters. Linear regressions were used to investigate the relationship between the relative abundance of MGI/MGII and environmental variables; a Wilcoxon test was used to investigate whether these same groups had different abundances at high vs low tide.

R packages used were as follows: agricolae (de Mendiburu 2021); colorBlindness (Ou 2021); ggplot 2 (Wickham 2009); grid (R Core Team 2021); gridExtra (Auguie 2017); indicpecies (De Cáceres et al. 2009); reshape (Wickham 2007); SRS (Beule and Karlovsky 2020); tidyverse (Wickham et al. 2019); timeSeries (Wuertz 2020); vegan (Oksanen et al. 2020); viridis (Garnier et al. 2021); and weathermetrics (Anderson et al. 2013).

## **2.5 Lipid extraction**

Lipids were extracted from glass fiber filters via a modified Bligh and Dyer method (Sturt et al. 2004, Bligh and Dyer 1959). Individual filters were removed from the freezer and placed in a combusted glass centrifuge tube with a 2:1:0.8 mix of methanol (MeOH), dichloromethane (DCM), and aqueous phase (first a phosphate buffer solution (P-buffer), then a 5% w/v trichloroacetic acid (TCA) solution). The tubes were sonicated for 20 minutes, then solvent was transferred to a separatory funnel and GenPure water and DCM added to separate the organic and aqueous phases. The organic phase was drained into a Labconco evaporation flask. The extract was then rinsed twice more with DCM, shaken, and the organic phase drained into the flask. Extracts were dried down to < 2 ml in a Labconco RapidVap under ultra high purity 5.0 grade N<sub>2</sub>, pipetted into pre-combusted

glass storage vials, given an N<sub>2</sub> headspace and stored in a -80°C freezer. It was determined that extracting a single filter likely would not yield sufficient lipid biomass to be detectable by mass spectrometry, so multiple filters were subsequently extracted together to create a pooled/combined extract for each sample. The process was similar to the above except centrifugation was used instead of a separatory funnel, and the organic phase was pipetted out of the bottom of the centrifuge tube after centrifuging at 5000 rpm for 5 minutes. For both methods, extracts containing both aqueous phases (P-buffer and TCA) were combined.

## Chapter 3

### RESULTS

#### 3.1 Physical and Chemical Parameters

Physical and chemical parameters measured using the YSI ProSolo probe (temperature, dissolved oxygen, salinity, and total dissolved solids, Figure 1) were carried forward in the analysis and used to determine if they were correlated with aspects of the archaeal community structure. There was an expected seasonal trend in temperature and salinity fluctuated with the tides. Per Pearson's correlation coefficient, temperature and dissolved oxygen were highly negatively correlated ( $r^2 = -0.93$  for 0 m - 0.94 for 1 m) and salinity and total dissolved solids were highly positively correlated ( $r^2 = 0.99$  for both 0 m and 1 m). No other combinations of variables had high or moderate correlations.

PAR data was collected for the entire time series with a few missing dates due to instrument malfunction. However, these data were not carried forward for analysis because it became clear they were influenced dramatically by short-term phenomena such as passing clouds or shadows from the dock, and thus were unlikely to be meaningful when related to community dynamics. Samples were collected for the measurement of nitrite, nitrate, DIC, and DOC, but only a subsection of samples for the latter two have been analyzed so far. See Table B.2 for these ancillary data.

Total chlorophyll from the entire time series was measured, but these data were not carried forward for analysis. Large differences between concurrent samples taken

from 0 meters and 1 meter depth were observed which was unexpected given the well-mixed nature of the study site (DeWitt and Daiber 1973) and the similarity between other values such as temperature and salinity at the two depths. The high variability cannot be explained by the measurement uncertainty as uncertainty is small compared to the difference between 0 and 1 meter pairs for each sampling event; the difference in chlorophyll values between 0 and 1 meters could be as much as 7.6  $\mu\text{g/L}$  for the same sampling event. Because our sampling volumes were larger than typical chlorophyll samples, uncertainty may have been introduced in the dilution of the samples. The fact that the chlorophyll values that we measured were lower than those typically reported for the Delaware Bay (DNREC et al. 2022) (measured values were always less than 10  $\mu\text{g/L}$ , and often less than 1  $\mu\text{g/L}$ , compared to a mean value of 15.14  $\mu\text{g/L}$  for DNREC historical data from the same site), indicates that it is possible that noise in the measurement overwhelmed the signal (Figure A.5). Regardless of the cause of the variability in total chlorophyll, we suspect it may not represent true chlorophyll concentrations in the Broadkill River. Instead of the measured chlorophyll data, averaged historical chlorophyll A data from the same sampling location (DNREC et al. 2022) were considered when explaining trends in archaeal diversity.

### **3.2 DNA Yield**

Total DNA extracted from filters was quantified with a Nanodrop. The 0 m GF/D filter from July 21, 2020 was an outlier with a DNA concentration an order of magnitude higher than any other sample. Sequence data from this sample were similar to the sample taken at 1 meter and samples from the month before and therefore did not seem to be

biased by contamination. It is most likely that this high concentration represented an erroneous measurement from the Nanodrop therefore this sample was removed prior to creating Figure 6, which shows DNA concentrations across the time series and box plots created with these data separated by filter pore size (and therefore particulate size fraction). A Tukey's HSD test revealed that DNA yield was lower in the colder months (October-March) than in the warmer months (April-September). The 2.7  $\mu\text{m}$  and 0.22  $\mu\text{m}$  pore size filters were not different in terms of DNA concentration, but the 0.7  $\mu\text{m}$  pore size filters had significantly lower DNA concentrations than the other two. This corresponds with a pattern visible from rarefaction curves, where the largest and smallest pore size yielded more OTUs than the smallest pore size (Figure 2). This difference is significant per a Tukey's HSD test and indicates a bimodal distribution of archaeal biomass in the largest ( $> 2.7 \mu\text{m}$ ) and smallest (0.22 – 0.7  $\mu\text{m}$ ) size fractions.

### **3.3 Relative Abundance of Classes**

Normalized data were plotted in stacked bar charts to visualize the changing abundance of the archaeal classes present in the Broadkill River (Figures 3-5). There was a clear distinction between the distribution of archaeal groups that were most abundant in the largest ( $>2.7 \mu\text{m}$  GF/D filter) and medium size fractions (2.7 – 0.7  $\mu\text{m}$  GF/F filter) compared to the smallest size fraction (0.7 – 0.22  $\mu\text{m}$  nucleopore filter). In the two larger size fractions, the groups Halobacterota/Halobacteria, four methanogen taxa (Methanomicrobia, Methanobacteria, Methanocellia, and Methanosarcinia), and an unclassified Crenarchaeota group are abundant (represent  $>5\%$  of the community). Bathyarchaeia become most abundant in the largest fraction in June at low tide (0 meters)

and in April at high tide (1 meter). Halobacteria makes up >5% of the community only in the medium size fraction (GF/F) in December at low tide (both depths) November at high tide (1 meter). In fact, the high abundance of Halobacteria in the medium size fraction in December represents a unique event given that it was never abundant at any sampling dates except November. An unclassified group in the phylum Halobacterota appears in December at low tide in the largest size class at both depths, but no unclassified Halobacteria make up more than 5% of the community elsewhere. Either one or several classes of unclassified Crenarchaeota are present in the two larger size fractions but not in the smallest size fraction. Nanoarchaeia, Thermoplasmata, Nitrososphaeria and unclassified Archaea are the only groups that represent more than 5% of the community in all three size fractions (though not necessarily every sample) and the only groups present in the smallest, 0.22 – 0.7  $\mu\text{m}$  fraction.

The relative abundance of all four abundant methanogen classes were negatively correlated with the relative abundance of Thermoplasmata (MGII) in the two largest size classes and at both depths, with the exception of Methanosarcinia, for which this correlation was only present in the largest size fraction (Table B.3). This is unsurprising given that the highest abundance of Methanosarcinia was observed in the largest size fraction and it was often <5% in the smaller size fractions. The relative abundance of Methanobacteria was positively correlated with that of Methanocellia in the two larger size fractions at both depths. Relative abundance of Nitrososphaeria (MGI), Thermoplasmata (MGII) and the sum of all methanogens over time are plotted in Figure 7. The results of linear regressions of these groups and their relationship to environmental

variables are summarized in Table 2. MGI had no correlations with any environmental variables except in the largest size fraction, where it correlated positively with salinity and TDS. MGII correlated positively with salinity, temperature, and TDS, and negatively with dissolved oxygen. Methanogen relative abundance correlated positively with TDS, salinity, and temperature, and negatively with dissolved oxygen.

### **3.4 Alpha Diversity**

The Shannon-Wiener diversity index was used to investigate alpha diversity, with a Tukey's HSD test employed to determine which groupings had significantly higher or lower diversity than others (Figure 8). Alpha diversity was higher in samples taken at low tide than in samples taken at high tide. No significant difference was found in alpha diversity between samples taken at 0 m vs 1 m. When comparing particulate size fractions, the Shannon-Wiener index indicated that the samples collected on the 2.7  $\mu\text{m}$  pore size filter were more diverse than the 0.7  $\mu\text{m}$  pore size samples, which were more diverse than the particulate matter collected on 0.22  $\mu\text{m}$  filters. There was no difference between spring and winter samples, but both were more diverse than fall samples which in turn were more diverse than summer samples. The highest diversity was observed in the largest size fraction in samples taken at low tide in the winter and spring and the lowest diversity was observed in the smallest size fraction in samples taken at high tide in the summer.

### **3.5 Indicator Species Analysis**

The results of the indicator species analysis test show which classes are more available in which categories (Table 3). Notably, Thermoplasmata and Nitrososphaeria were both more abundant at high tide than at low tide. Thermoplasmata was most abundant in the largest size fraction and was more abundant in summer and fall than winter and spring. Nitrososphaeria was more abundant in the middle and smallest size fractions compared to the largest and had no apparent seasonal trend. There were similarities between all four abundant methanogen classes (Methanomicrobia, Methanobacteria, Methanocellia, and Methanosarcinia). All were more abundant in the winter and spring than in the summer and fall. All were most abundant in either the largest size class (Methanosarcinia and Methanomicrobia) or the two largest size classes (Methanocellia and Methanobacteria). While not entirely absent from the smallest size class, no class of methanogen ever made up more than 5 percent of the community, and in most cases represented less than 1%. Only one class, Thermoprotei, was more abundant at one depth (0 m) than the other. Table 3 also shows some of the less abundant classes that never made up more than 5% of the population but nonetheless were detected and observed to be correlated with a size class of particles or environmental variable.

### **3.6 Explanatory Variables**

The stress value for the ordination used to produce NMDS plots was 0.14, indicating an acceptable representation of the data as it lies below the threshold of 0.2 for acceptability (Dexter et al. 2018). Figure A.6 shows a stress plot of the ordination used

for all NMDS plots. Overall, based on visual analysis of NMDS plots, the community structure was most different between the size fractions (represented by GF/D, GF/F, and nitrocellulose (Nit) filters) (Figures 9 & 10). Visual analysis of NMDS plots show that community structure was not different based on depth, a finding confirmed by a non-significant ANOSIM result (Table 4).

NMDS plots, based on the Bray-Curtis dissimilarity matrix, provide insight into the factors that influence the community structure of the Broadkill. There is no apparent separation at all based on depth, which is supported by insignificant ANOSIM p-value. An ANOSIM R-statistic of  $< 0.25$  indicates that samples are not separable based on tide, and that there is a high degree of overlap in the samples taken at high vs. low tide (Ramette 2007). Likewise, comparing samples separated by season resulted in an ANOSIM R-statistic of  $< 0.25$ , indicating that samples are not separable based on season. The seasons were grouped in three-month blocks as follows: winter (Dec-Feb); spring (Mar-May); summer (Jun-Aug); and fall (Sep-Nov). As these groupings were relatively arbitrary, the groupings were shifted forward and backward by one month and ANOSIM were re-run as a sensitivity analysis. No change in interpretation of the data resulted from this; samples were still not separable by season. The year was also split into two halves, winter/spring (Dec-May) and summer/fall (Jun-Nov), a distinction that can be seen plotted on an NMDS (Figure 10). This split was made because the NMDS plot with samples colored by season appeared to have winter and spring samples grouped together, and likewise with summer and fall samples. An ANOSIM R-statistic of  $> 0.25$  indicates that samples are indeed separable by this grouping, but with overlap. The same sensitivity

analysis as above was performed on this grouping; when it was shifted later by one month, the samples were no longer separable per ANOSIM; when shifted one month earlier (Nov-Apr and May-Oct), they were.

The clearest separation of samples is based on pore size, indicating that samples collected on different filter pore sizes represent distinct archaeal populations. This is supported by an ANOSIM R-statistic of 0.45, indicating the samples are different in different particulate size classes but with some overlap. The ANOSIM test also indicates that, based on the high R-statistic (0.72), the greatest difference is between the largest and smallest particles (samples from GF/D and nitrocellulose filters). Figure 10 shows environmental vectors fit onto the ordination plot and Table 5 shows the R<sup>2</sup> and p-values for each according to a Mantel test. All environmental variables (salinity, temperature, dissolved oxygen and total dissolved solids) had significant Mantel p-values, but the R statistics indicated they did not explain very much of the variation when all samples are taken together.

In order to determine whether some archaeal populations in different particulate size classes respond to environmental variables independently from each other, NMDS plots and statistical tests were recreated on samples from each size class separately. See Figures A.7 and A.8 for NMDS plots produced via this method. Non-parametric statistical tests performed separately for each pore size yielded different results in a few cases, suggesting the portions of the community represented by different size fractions might respond differently to environmental parameters. Whereas when considering all samples together, samples were not separable by season, ANOSIM tests performed on

pore sizes individually revealed that the samples taken at different seasons were indeed separable (but overlapping) for each size class taken on its own, with higher separability seen in the larger two fractions (Table B.4). As with all samples together, samples were separable by the winter/spring and summer/fall split, again with this effect more pronounced in the larger two size fractions. Correlation with salinity, temperature, dissolved oxygen, and TDS was low (based on Mantel test) with individual size classes as with the total population combined, with the exception of a modest r-value for temperature for the largest size fraction (Table B.5). Alpha diversity patterns were similar to those seen when all size fractions were considered together (Figure A.9).

## Chapter 4

### **DISCUSSION**

The goal of this study was to investigate the diversity and phenology of the planktic archaeal community in a tidal estuarine system over the course of a year, with a focus on the effects of season, tidal stage, particle size, primary productivity and light availability. In addition to direct measures for some of these parameters, proxies such as temperature, salinity, and chlorophyll concentration were also used although not all proxies were as representative of environmental conditions as I anticipated. For example, PAR did not clearly distinguish between 0 meters and 1 meter depth in the turbid water column of the Broadkill River and was sensitive to artifacts related to weather, shadows and cloud cover. Therefore the hypothesized relationship between light availability and MGII abundance was not evaluated. Robust indicators for season, tidal stage and particle size, however, were found.

Determining which factors shape diversity in a community can help explain the way the community functions. Because microbes play such important roles in marine biogeochemistry, measuring their diversity and identifying taxa can inform us about the biogeochemical processes mediated by archaea in the environment (Strom 2008). Alpha diversity itself can tell us about the community as well without the need for metagenomic sequencing targeting functional genes; a more diverse community likely has more niches present and a wider array of metabolic strategies than a less diverse community. This

study considers both alpha diversity, a measurement of diversity in an individual sample, and beta diversity, a measurement of diversity across all samples.

#### **4.1 Factors Explaining Community Structure**

With this study, we wanted to understand which factors were driving the overall diversity in the archaeal community as well as which were affecting individual taxa. It was found that factors which did not explain overall diversity may still explain the changes in abundance of particular taxa. The most important factor explaining differences in overall community structure was size class as shown on NMDS plots (Figure 9) and ANOSIM results (Table 4). This, and the higher alpha diversity in the larger particle size classes, reveal a divide between larger particle-associated archaea and archaea that are presumably free-living in the sub-micron size class, indicating that these communities are quite different from each other. The NMDS plot (Figure 9) shows some similarity between the two largest (GF/D and GF/F;  $>2.7 \mu\text{m}$  and  $0.7 - 2.7 \mu\text{m}$ ) size fractions but a separate smallest (Nitrocellulose;  $0.22 - 0.7 \mu\text{m}$ ) size fraction, suggesting that the true divide is bimodal, i.e. there is likely a community associated with particles less than  $0.7 \mu\text{m}$  in diameter and a smaller, sub-micron community that is likely free-living, rather than a continuum of particle sizes and archaeal cells attached indiscriminately to all sizes of particles. This is supported by the amount of DNA extracted the different filter types, which shows higher DNA concentration in the largest and smallest size fraction than the middle size fraction (Figure 6). Many studies that sample marine planktic archaea do not capture particles and cells smaller than  $0.7 \mu\text{m}$  (Molina et al. 2020; Turich et al. 2007; Wuchter et al. 2005). These studies likely misrepresent the free-living community by

failing to capture the some of the small, free-living biomass. The high concentration of DNA on the smallest filters indicates that a significant proportion of the community would be lost by using a filter that is not capable of capturing the  $< 0.7 \mu\text{m}$  fraction. The sub-micron fraction of plankton cells and POM is generally understudied and often ignored but is an important component of the marine biological carbon pump (Close et al. 2013).

This study reinforces the importance of particle association for estuarine planktic archaea. One study of an estuary found a higher diversity in particle-associated than free-living bacterioplankton (Crump et al. 1999), which is consistent with this study's findings. However, a pelagic study found the opposite, i.e. the free-living microbial community (both bacteria and archaea) was more diverse than its particle-associated counterpart (Kellogg and Deming 2009). Because sediment is entrained in the water column in shallow environments like estuaries (Crump et al. 1999), it is possible that many of the particle-associated archaea detected in this study originate from sediment and therefore have a different composition than pelagic particles. The seeding of microbes from a distinct environment could explain the higher diversity of particle-associated microbes in estuaries than the open ocean, where the water column to sediment relationship tends to only go one way -- i.e., particles from the water column may transport pelagic microbes to the sediment, but not vice versa (Mestre et al. 2018).

Time of year was also found to have an influence on archaeal community composition. While season and temperature were hypothesized as important factors, dividing the year in half was more effective. The significance of the summer/fall and

winter/spring divide in structuring the community reflects the location of the study site. Delaware has a temperate climate with dramatically different seasons, so a seasonal component to the data was not unexpected. The low diversity in summer appears to be driven by Thermoplasmata, which represented the majority of the community in June and July, matching the high proportion of Thermoplasmata seen in July by Yoshimura et al. (2018). Time series data from more locations and spanning several years would do much to elucidate the drivers of the abundance of archaeal taxa.

To my surprise, tidal stage and salinity were not strong drivers of archaeal community composition. Few studies have examined tidal stage as a driver of changes in an archaeal community. The goal of sampling at low and high tide was to compare the marine and riverine endmembers, with the expectation that the marine endmember assemblage would resemble that of a coastal ocean water column. In general, samples were not separable by tide, but as discussed below, tide (and salinity, which can be considered a proxy for tidal stage) affected the abundance of certain key taxa. If high tide is taken to represent the marine endmember, we would expect to see a community similar to those observed in pelagic water column environments, which have less diverse archaeal assemblages than riverine water column environments (Chen et al. 2019, Anas et al. 2021). As expected, it was observed that diversity was lower at high tide and higher at low tide, the likely reason being the greater abundance of anaerobic archaea such as methanogens at low tide. Particle-associated anaerobic microbes have been found to be more abundant at upriver than downriver sites within a single estuary (Chen et al. 2019, Yoshimura et al. 2018), so the higher diversity at low tide can be attributed to the greater

abundance of these groups, since low tide represents the riverine endmember at the Broadkill River mouth. These groups are likely present as the result of sediment entrained in the water column as the tide goes out. Sediment particles can remain suspended in a turbid estuary for 2-4 weeks, suggesting that a stable community of particle-associated microbes that could form and play a consistent ecological role at our site (Crump et al. 1999).

#### **4.2 Nitrososphaeria (MGI)**

The experimental design of this study was designed to test the hypothesis that archaeal community would be different during the river-influenced low tides and more marine-influenced high tides. We hypothesized that MGI would be more abundant under higher salinity conditions and greater marine influence (associated with high tide) as seen in Chen et al. (2019). Relative abundance of MGI and MGII shows higher MGI abundance at high tides than low tides in the largest size fraction (Figure 7); a Wilcoxon test comparing MGI abundance at low and high tide confirms this pattern (Table 2). This differential tidal effect between the size fractions could be due to tides bringing in particles with MGI in from the Bay; the free-living fraction may not be as influenced by the tides. The greater relative abundance of this group in the two smaller size fractions, however, suggests a larger proportion of the detected MGI were free-living and not affected by tidal stage or salinity. The tidal association of MGI abundance seen in large particles is not unexpected, as this group is typically associated with the pelagic water column (Santoro et al. 2019); the lack of this association for the free-living fraction may mean that the particle-attached community shifts more with the tide than the free-living.

The positive correlation of MGI relative abundance with salinity is likely related to this relationship with the tides. Indicator species analysis suggests MGI was more abundant in the smaller size fractions, but previous studies suggest that MGI has no preference for a particle-associated over a free-living lifestyle (Jain and Krishnan 2021); MGI were indeed present at >5% of the community in all three size fractions in this study. The lower abundance in the largest size fraction may be attributable to the higher proportion of methanogens in that fraction, as is discussed in the next section.

The presence of MGI nearly year-round at this site suggests the group plays an important role in ammonia oxidation in estuaries, as it does in the open ocean (Pester et al. 2011), which would be corroborated by nitrite and nitrate quantification. Historical data shows no trend in total nitrogen at the sampling site (DNREC et al. 2022), but there may be a trend in nitrite or nitrate that is obscured by the measure of total nitrogen. Unlike for most of the abundant taxa detected in this study, no clear seasonal difference was observed in the relative abundance of MGI. Some studies have reported that MGI abundance peaks in winter (Wuchter 2006, Herfort et al. 2007, Galand et al. 2010, Hugoni et al. 2013), whereas others do not (Pernthaler et al. 2002, Quiñones et al. 2009). Murray et al. (1999) noted a negative correlation of prokaryote abundance with MGI abundance, suggesting MGI is most abundant when overall microbial abundance is low. The productive and diverse nature of the estuarine environment may prevent MGI from ever becoming dominant over other taxa.

### 4.3 Thermoplasmata (MGII)

Given their hypothesized heterotrophic metabolism and light harvesting capabilities (Frigaard et al. 2006), I hypothesized that MGII archaea would show a preference for seasons with more light availability and a possible correlation to indicators of phytoplankton productivity such as chlorophyll and DOC concentrations.

Thermoplasmata (MGII) showed a higher relative abundance in summer and fall and at high tide. The higher abundance at high tide suggests a preference for higher salinity marine conditions, which is consistent with reports from the Cochin estuary in India (Anas et al. 2021), the Pearl Estuary in China (Chen et al. 2019), and the Broadkill River (Yoshimura et al. 2018). The seasonal trend could be explained by a number of factors. Many studies have observed MGII blooms in summer (Pernthaler et al. 2002, Wuchter 2006, Herfort et al. 2007). One potential explanation that has been given in temperate or polar locations could be that longer day lengths (and therefore more available sunlight) support the growth of photoheterotrophic MGII phylotypes (Frigaard et al. 2002). However, higher relative MGII abundance lasted into the fall. During the spring, when day lengths were comparable to the fall through October when day lengths are much shorter, relative abundance of MGII was lower. Longer day lengths may have played a role in kickstarting the bloom, but additional factors are necessary to explain their persistent high abundance through the fall.

Many studies link MGII blooms to phytoplankton blooms, often using chlorophyll concentrations as a proxy. In the North Sea, MGII blooms have been found to correspond directly with an increase in chlorophyll concentration/phytoplankton bloom (Herfort et al.

2007, Orellana et al. 2019). In another North Sea study (Wuchter 2006), and in offshore California (Needham and Fuhrman 2016, Murray et al. 1999), MGII blooms have been found to occur after a phytoplankton bloom, with lags ranging from a few days to about a month. The relationship between MGII abundance and phytoplankton blooms is attributed to the probable reliance of MGII on high molecular weight organic compounds deriving from phytoplankton (Iverson et al. 2012, Orsi et al. 2015). A goal of this study was to investigate the association of MGII abundance with phytoplankton in the context of an estuary using chlorophyll concentrations as a proxy for the summer phytoplankton bloom. Unexpectedly, historical data from the last 20 years from the mouth of the Broadkill (DNREC et al. 2022) shows no statistically-significant seasonal trend in chlorophyll A concentrations (Figure A.4). These data support the lack of a seasonal trend that we observed in our own total chlorophyll concentrations when monthly measurements from 0 and 1 meters depth are averaged together (although they do not explain the variability between depths that we report) (Figure A.8). It may be that our monthly chlorophyll values do not have sufficient time resolution to capture a summer phytoplankton bloom in 2020 and 2021. Alternatively, the absence of a summer maximum in total chlorophyll concentrations may be due to efficient zooplankton grazing. A similar absence of a chlorophyll (in this case total chlorophyll) peak observed at the mouth of the Delaware Bay by Voynova et al. (2013). In fact, chlorophyll concentrations decreased slightly in the summer in that study although a summer peak was reported from independently-measured primary production. The authors found that zooplankton biovolume increased at the same time as this increase in primary production

and suggested that this allowed for an efficient transfer of phytoplankton carbon to primary consumers such that chlorophyll did not represent the increase in primary production. If similar dynamics occur at the mouth of the Broadkill River, efficient zooplankton grazing could explain the lack of a seasonal chlorophyll peak. Chlorophyll *a* is widely considered to be a good proxy for phytoplankton biomass (Huot et al. 2007), but our data and historical data from the Delaware Water Quality Portal indicate that it does not appear to accurately reflect phytoplankton activity at the Broadkill River outlet and lower Delaware Bay (Voynova et al., 2013, DNREC et al. 2022). Based on the results of Voynova et al. 2013, a seasonal increase in the availability of phytoplankton-derived organic carbon could still occur, driving an MGII bloom despite this not being reflected in the chlorophyll data. Future studies at this site could directly measure primary production or the abundance of phytoplankton sequences to test this hypothesis.

A confounding factor in interpreting the data of the relative abundance of MGII is the existence of multiple phylotypes that occupy different niches. Galand et al. (2010) and Hugoni et al. (2013) identified MGII.a and MGII.b, the former of which bloomed in the summer in their studies, the latter in the winter. Our sequence data indicate a population of MGII that blooms in the summer which may indicate a dominance of just one niche occupied by MGII and possibly one phylotype. This pattern was also observed by Orellana et al. (2019), who noted the different metabolic capabilities of MGII.a and MGII.b, the latter of which has a smaller, more streamlined genome and adaptations to survive in the absence of phytoplankton blooms such as a sulfur assimilation pathway. In a river-influenced setting with high DOC concentrations such as the Broadkill, the

adaptations of MGII.b have for survival under conditions of lower organic carbon supply may be less advantageous. Orellana et al. noted that summer blooming MGII.a cells are smaller than MGII.b cells, an adaptation that could help them avoid grazing and also could also explain why the summer MGII bloom in this study is the most pronounced in the smallest size fraction (0.7 – 0.22  $\mu\text{m}$ ). Given that relatively few phylotypes of MGII dominate globally (Massana et al. 2000), it is possible that the summer bloom of MGII observed at the mouth of the Broadkill River can be attributed to MGII.a. Unfortunately, the short sequence length resulting from a sequencing error does not allow for phylotype-level specificity to be determined from our OTUs. A future sequencing run could result in higher quality sequences that can distinguish between the two phylotypes.

Other factors that have been identified as contributing to MGII blooms in other settings can likely be ruled out. Galand et al. (2010) attributed the summer MGII.a bloom in the Mediterranean Sea to stratification of the water column; however, this does not occur in the Broadkill (Dewitt and Daiber 1973). Murray et al. (1999) specifically investigated whether the availability of nutrients like nitrite, nitrate and phosphate affected MGII blooms, and did not identify any strong relationships like those consistently observed for MGI. Needham and Fuhrman (2016) identified particular phytoplankton taxa whose abundance correlated with that of MGII. We cannot evaluate this possibility without sequencing DNA amplified with 18S primers which was beyond the scope of this project. However, a future investigation of the eukaryote community in the Broadkill River might reveal similar results. The occurrence of a summer MGII bloom at this study site in three different years (2020 and 2021, measured in this study,

and in 2014, as reported by Yoshimura et al. 2018), suggests the driver of this bloom reoccurs annually in June. We have determined that the MGII bloom cannot be correlated with hours of daylight, temperature or chlorophyll concentrations individually. More work is needed to determine its precise cause.

MGII had higher relative abundance in the smallest size class, but was present in all three at >5% of the community. Some MGII phylotypes appear to have a preference for particle-associated lifestyles; others are more abundant in free-living fractions, but most have no preference either way (Jain and Krishnan 2021). There may be an abundant phylotype with a preference for a free-living lifestyle in the Broadkill; alternatively, its higher relative abundance in the smallest size class may be attributable to lack of methanogens and other archaeal classes in that fraction.

#### **4.4 Methanogen Classes**

Several methanogen classes were detected in this study, and all were more abundant in the larger size fractions and found only in very low abundance in the smallest size fraction. This likely has to do with their metabolic strategy. Methanogenesis is inhibited by oxygen and so these methanogens are strictly anaerobic (Offre et al. 2013); they would not be able to metabolize as free-living individuals in an oxic water column such as that of the Broadkill River. However, some methanogens are able to take advantage of the hypoxic or anoxic interiors of particles (Simon et al. 2002). The probable particle-associated lifestyle of water column methanogens may explain their near absence from the smallest size class. Particulate material captured on 2.7  $\mu\text{m}$  GF/D

filters appeared brown suggesting the presence of large quantities of re-suspended sediment. Methanogens are the predominant microbes in estuarine sediment (Biddle et al. 2006), so the methanogens captured from the water column may have their origin in sediment that gets entrained in the water column. (Chen et al. 2019), in their study of archaeal diversity in the water column of the Pearl River Estuary, found a higher abundance of methanogens in bottom waters than surface waters, lending credence to the theory that these archaea have their origin in sediment.

The higher abundance observed for all abundant methanogen classes in winter and spring compared to summer and fall is a surprising finding that does not appear to be widely reported in the literature or expected given that methanogens with a sediment source would be expected to reflect abundance in the sediment and archaeal diversity in sediments is unlikely to have a seasonal pattern. While there is a significant correlation between the sum of the relative abundance of methanogens and temperature (Table 2), temperature is unlikely to be the cause of their lower abundance during the summer and fall as methanogens are not inhibited by warm temperatures. In fact, methanogens in aquatic sediment have been found to have higher activity at higher temperatures (Zeikus and Winfrey 1976). Notably, MGII and methanogens are anti-correlated in the large and medium particles and a pronounced bloom of MGII occurs in June. Given that we did not amplify archaeal DNA by quantitative PCR (qPCR), a more likely explanation may be that the bloom of Thermoplasmata (MGII) in the summer and fall may have obscured the methanogen population in our results. It would be possible for the absolute abundance of the methanogens to remain the same year-round, but if the absolute abundance of MGII

increased in summer, the relative abundance of methanogens would decrease as we report; in other words, the signal from increasing MGII abundance may be drowning out a relatively stable methanogen community. However, these results do not distinguish between a seasonal pattern in methanogen abundance and a decrease in relative abundance due to an increase in absolute abundance of MGII. Sampling at this site but amplifying DNA via qPCR would help resolve this question.

There were unique aspects to the relative abundance patterns of each of the abundant methanogen taxa. Methanocellia and Methanobacteria were more abundant at low than high tide (Table 3). This is not unexpected, as Chen et al. (2019) reported higher methanogen abundance at more lower salinity riverine sites than higher salinity marine sites in their study of an estuarine salinity gradient. Moreover, at least one cultivated representative of the order Methanocellales is reported to have lower salinity tolerance than Methanosarcinales. The reported maximum salinity tolerance of Methanocellales is 20 ppt (Sakai and Imachi 2016), compared to greater than 33 ppt for Methanosarcinales (Sowers and Gunsalus 1998). This could explain Methanocellia's affinity for low tide. Several cultured representatives of Methanobacteriales, however, had a salinity tolerance similar to that of or exceeding Methanosarcinales (Ciulla et al. 1994, Shlimon et al. 2004). However, Yoshimura et al. (2018) found Methanobacteriales in higher abundance in upriver sites, so the phylotype(s) found in the Broadkill may be less salinity-tolerant. Alternatively, the presence of more suspended particles upriver than downriver in the Broadkill River (Dewitt and Daiber 1973, Yoshimura et al. 2018) could accommodate larger populations and be the reason for their greater abundance at low tide. The relative

abundance of Methanocellia and Methanobacteriales in this study were positively correlated, and Methanocellia was only detected in abundance when Methanobacteriales was as well. These similarities suggest a degree of niche similarity between the two, which is supported by their evolutionary relatedness (both are Class I methanogens) (Adam et al. 2017). Both are hydrogenotrophic (Bonin and Boone 2006, Sakai et al. 2011), so perhaps increase in abundance when H<sub>2</sub> or formate become more available.

Methanomicrobia, the most abundant methanogen taxon at this site, is hydrogenotrophic like Methanobacteria and Methanocellia (Garcia et al. 2006). One reason it may be more abundant than those groups is the ability of archaea in that clade to efficiently use low concentrations of H<sub>2</sub>, which they use as an electron donor to reduce CO<sub>2</sub> into CH<sub>4</sub> (Anderson et al. 2009). This may give them a competitive edge over other methanogens with less affinity for low concentrations of H<sub>2</sub>. There is also a species of Methanomicrobia, *Methanotherix paradoxum*, that is globally abundant in oxic wetland soils and capable of managing oxic stress (Angle et al. 2017); this species or similar could be present in the Broadkill and dominate because of this unique ability, but with this study's data it is impossible to say. Methanomicrobia was also the most abundant methanogen detected in the Broadkill by Yoshimura et al. (2018), suggesting that conditions in the Broadkill River selects for their growth.

Methanosarcinia were found to represent >5% of the community from December through June, but only in the largest size fraction. Methanosarcinia have some of the largest archaeal genomes (Buan 2018) and are capable of the largest diversity of methanogenic pathways. Unlike the other three methanogen taxa, Methanosarcinales are

capable of all three known types of methanogenic metabolic strategies: hydrogenotrophic, acetoclastic, and methylotrophic (Kendall and Boone 2006). This makes Methanosarcinales the most catabolically diverse methanogen clade, and the only one that can split acetate to form CO<sub>2</sub> and CH<sub>4</sub> (Ferry and Lessner 2008). This means that they have access to substrates not utilized by other methanogens, making them a dominant clade in many environments (Kendall and Boone 2006). Acetate is a common intermediate in organic carbon mineralization in the marine water column (Zhuang et al. 2019), so use of acetate by Methanosarcinia could explain their abundance in the large size fraction. Another question is why, unlike with the other taxa, the relative abundance of Methanosarcinia is so reduced in the middle size fraction. Methanosarcinales cells occupy a wide size range including strains that fall both above and below 2.7 μm, the nominal pore size of the largest (GF/D) filters used in this study (Kendall and Boone 2006) implying that they could only be accommodated in the interior of the largest size class of particles. A FISH microscopy study would be able to confirm or deny this hypothesis.

Flux from estuarine and shelf sediments is a significant contributor to the global flux of methane, a potent greenhouse gas, contributing about 75% of all oceanic emissions (Bange et al. 1994). The detection of methanogens by this study raises the possibility of methane flux from the water column itself, especially given that they are present at this site nearly year-round. Methanogenesis is known to occur in oxic water columns, but the magnitude of its contribution to atmospheric methane is uncertain (Bogard et al. 2014) and modulated by the activity of aerobic methanotrophs in the water

column. Without metatranscriptomic data it is not possible to say for certain whether they are actively metabolizing, but the suspension of particles in estuarine water columns for weeks or months suggests it is a possibility (Crump et al. 1999). Methanogens have been found in other studies of estuarine water columns (Tee et al. 2021, Chen et al. 2019), so water column methanogenesis may be a feature of estuaries. This is supported by Yoshimura et al. (2018) who found a higher abundance of methanogenic groups at upriver sites. Chen et al. (2019) found methanotrophic bacteria in association with methanogenic archaea in the water column and surmised that some methane may be oxidized back to CO<sub>2</sub> before it escapes to the atmosphere. In the future it would be interesting to investigate whether methanotrophic taxa from the same site correlate in abundance with the methanogens.

#### **4.5 Other Anaerobic Classes**

Nanoarchaeia is part of the phylum Nanoarchaeota, a phylum that is characterized by small cell size (Huber et al. 2002), which would explain its higher abundance in the smallest size fraction. Some Nanoarchaeota are endosymbionts (Jarett et al. 2018), and the potential association with hosts could explain their presence in the larger size fractions as well. Most of the Nanoarchaeia at this site were further classified as order Woesearchaeales; this group is indeed thought to be symbiotic with or parasitic of other microbes (Castelle et al. 2015). They are often present in anoxic waters and sediment (Sollai et al. 2018), and their presence here could suggest utilization of anaerobic interiors of host cells. The lack of seasonal pattern or association with tide for this class could indicate the presence of a cosmopolitan variety of hosts, allowing Nanoarchaeia to

be present in the water column year-round. Its presence in the smaller size fraction, however, suggests hosts that are free-living and relatively small in cell size.

Bathyarchaeota are quite common in estuarine water columns (Liu et al. 2018). They are also found in sediments where they may be involved in methane metabolism and acetogenesis. In the water column, they can also be found in suboxic and anoxic regions (Sollai et al. 2018). This reliance on low-oxygen environments suggests that, as with the methanogens, Bathyarchaeota in the water column may be utilizing anoxic particle interiors. They can be organo-heterotrophs or acetogenic autotrophs (Lazar et al. 2016); the lack of detailed taxonomic information on the Bathyarchaeota from this study makes it difficult to speculate on their metabolic activity. Regardless, they do not appear to be a dominant class in the Broadkill River, only representing >5% of the community for two months, and only in the largest size fraction.

A surprising finding was the presence of several classes within the Asgardarchaeota phylum, specifically Lokiarchaeota and Odinararchaeota. These anaerobic taxa are typically found associated with sediments (Bulzu et al. 2019) and are rarely if ever detected in the water column, so finding them in this study is quite unique. These classes were more abundant in the largest particle size, suggesting that they, too, are particle-associated.

#### **4.6 Unclassified Taxa**

A considerable proportion of the community could not be classified at all (OTUs labelled “Archaea\_unclassified”) or could only be classified to the phylum Crenarchaeota

("Crenarchaeota\_unclassified"). There were also sequences that could not be classified even to domain level ("Unclassified\_unclassified"); these represented less than 5% of the population in all but one sample. Evidence suggests that these groups may be genuinely novel taxa (i.e. not present in the SILVA database) as opposed to the result of sequencing errors. One piece of evidence for this is that these groups remained even after removing low-abundance OTUs. Another is that these groups correlate with particular variables. Crenarchaeota\_unclassified, for example, are more abundant in the largest size fraction, and are mostly absent from the smallest fraction, never making up more than 5% of the community. A group resulting from a sequencing error is unlikely to have such strong size partitioning, so it stands to reason that this study may have found an undescribed class in the phylum Crenarchaeota. Archaea\_unclassified were more abundant in spring, at low tide, and in the two smaller size classes, also suggesting that this designation may represent a novel taxon. The relatively low sampling effort for archaeal diversity in estuaries would make the presence of undescribed taxa unsurprising. Other studies (Anas et al. 2021, Viera et al. 2017) also found a high proportion of archaea that could not be classified when they sampled an estuarine water column. However, if these are indeed novel taxa, it is somewhat surprising that Yoshimura et al. (2018) did not report such an abundance of unclassified groups from the same site; however, this could be explained by the MGII bloom that was occurring during their sampling. These unclassified groups made up a smaller percentage of the community during the bloom seen by this study as well. Using the BLAST tool to search the sequences of randomly-chosen unclassified sequences brings up near-100% matches to uncultured archaea found by other studies

(e.g. Baumgartner et al. 2009, Quaiser et al. 2011, Swan et al. 2010, Ye et al. 2009), which supports the idea of these being genuine undescribed taxa. Interestingly, these studies come from a variety of habitats, including freshwater (Ye et al. 2009), marine (Baumgartner et al. 2009, Quaiser et al. 2011), and hypersaline (Swan et al. 2010).

It is important to note that, as described above, there were groups whose relative abundance correlated with parameters (e.g. tide, season) that did not explain diversity changes in the overall community according to statistical tests. Because the abundance of different taxa are driven by different variables, this makes it less likely that any single variable will explain shifts in community structure as a whole. Archaea, as with bacteria, occupy a diverse array of niches (Offre et al. 2013), and individual groups are worthy of investigation as to factors affecting their abundance, particularly in what is clearly the complex environment of an estuary.

## CONCLUSION

This study represents a unique dataset: a census the diversity of an archaeal community in an estuarine river over the course of a year that also compares the community at high tide vs. low tide. More so than any other factor, it was found that size class is the greatest determinant factor of community structure at the mouth of the Broadkill River. The higher diversity of archaea in larger size fractions suggests a robust particle-associated community, likely originating from sediment entrained in the water column. Many of the classes found may employ anaerobic metabolic strategies such as methanogenesis in the water column. The bloom of MGII in June represents an exciting opportunity to learn more about this uncultured group, including an investigation into its membrane lipids. This bloom could not be attributed to an increase in chlorophyll concentration as expected, but may still be the result of increased availability of phytoplankton-derived organic carbon. It is clear that the estuarine water column hosts a diverse and dynamic archaeal community that differs from that of the pelagic marine water column in structure and phenology. This study illuminates how a single sampling event cannot be considered as representative of a community year-round, and that there is much more to be learned about the phenology and biogeochemical roles of planktic archaea in an estuarine setting.

## FIGURES AND TABLES

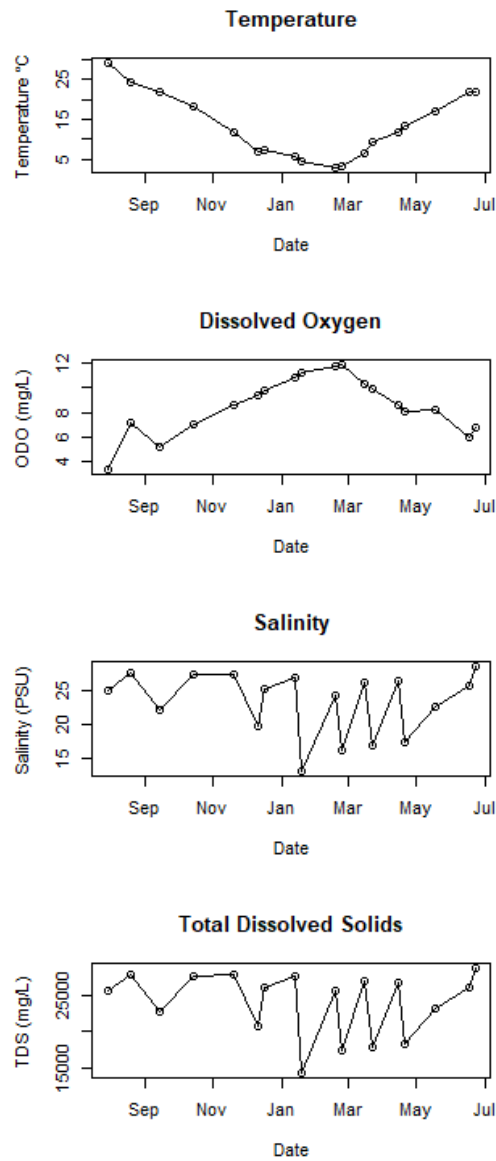


**Figure 1:** Time series of environmental data taken concurrently with water samples from July 2020 through June 2021 with YSI ProSolo probe. 0 m and 1 m data were almost identical so only 0 m data are represented here.

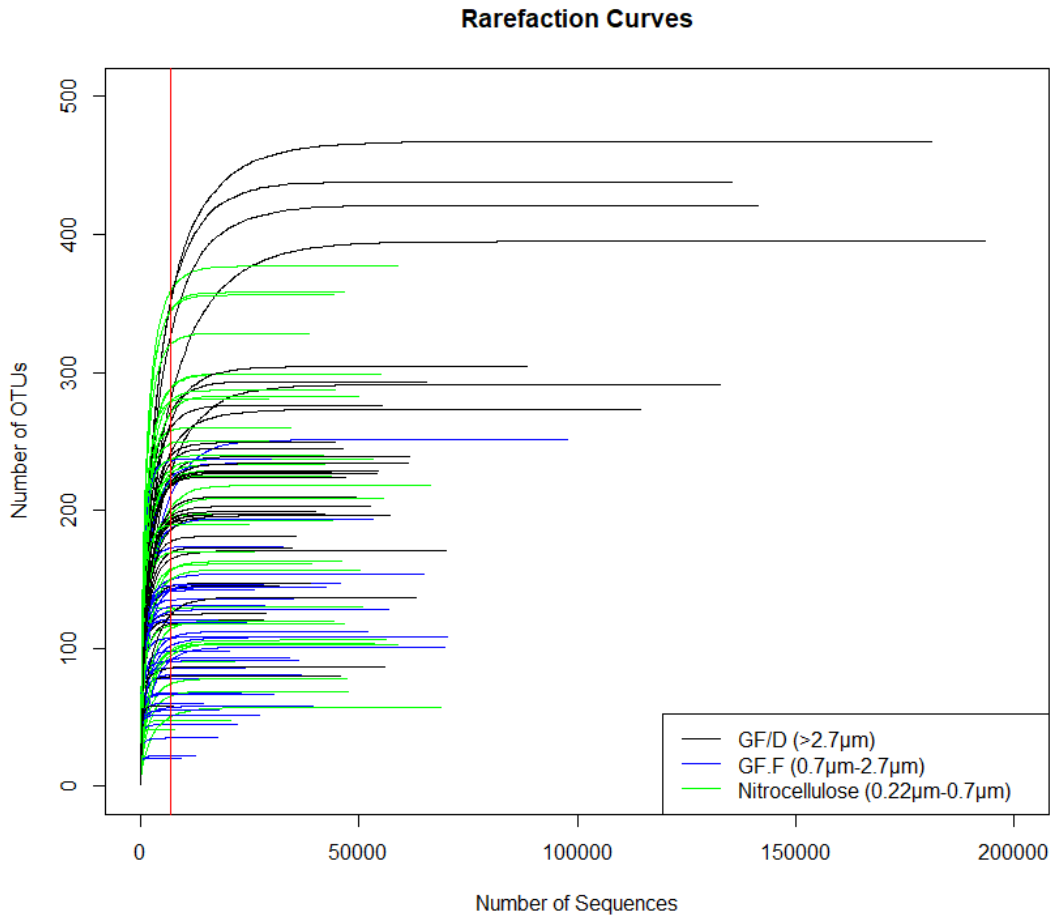


**Figure 2.** Rarefaction curves of all samples after removing low-abundance OTUs, color-coded by pore size. The vertical red line represents the cutoff value chosen for rarefaction of data (7000 sequences).

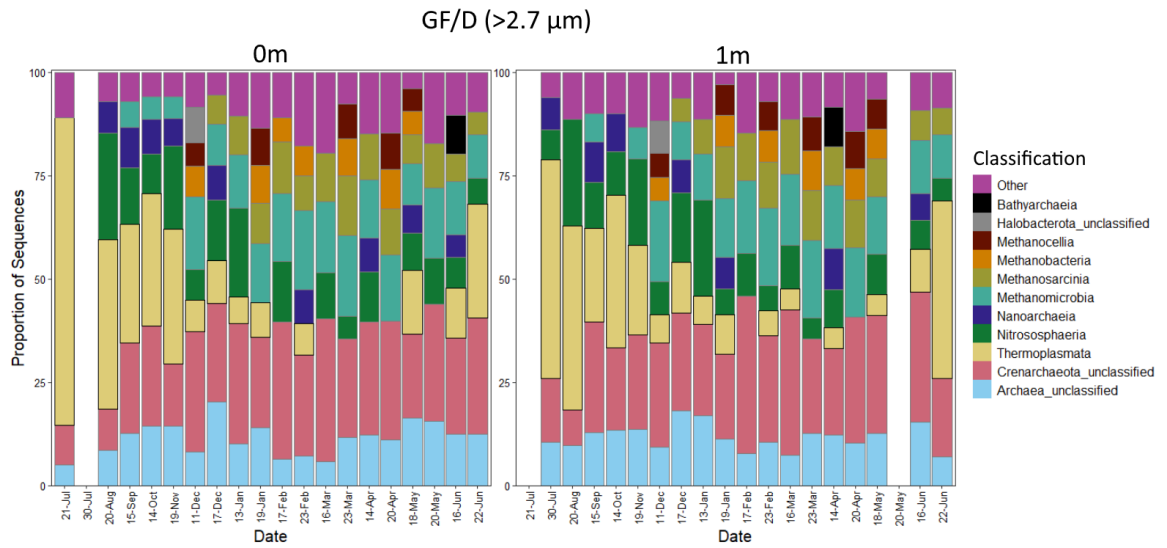


**Figure 3.** Community composition of archaea at the class level from the largest pore size (GF/D) filters at 0 m and 1 m depth representing particles  $>2.7 \mu\text{m}$ . Samples range from July 2020 to June 2021. Data are normalized by scaling with ranked sampling. The “Other” category contains all classes that represent less than 5% of the total community in that sample.



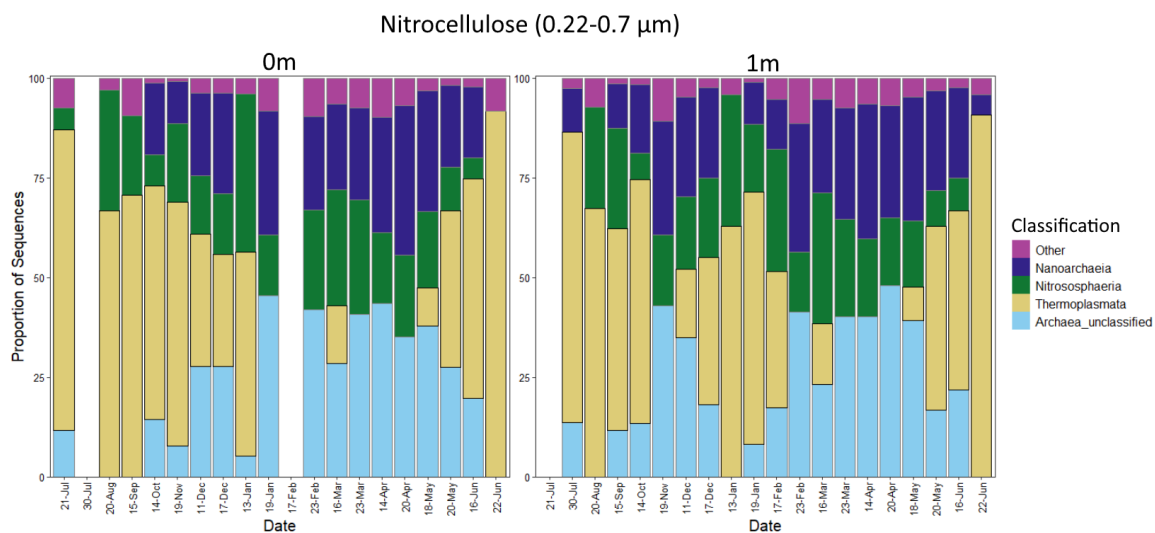


**Figure 5.** Community composition of archaea at the class level from the smallest pore size (nitrocellulose) filters at 0 m and 1 m depth representing particles from 0.22  $\mu\text{m}$  to 0.7  $\mu\text{m}$ . Samples range from July 2020 to June 2021. Data are normalized by scaling with ranked sampling. The “Other” category contains all classes that represent less than 5% of the total community in that sample.

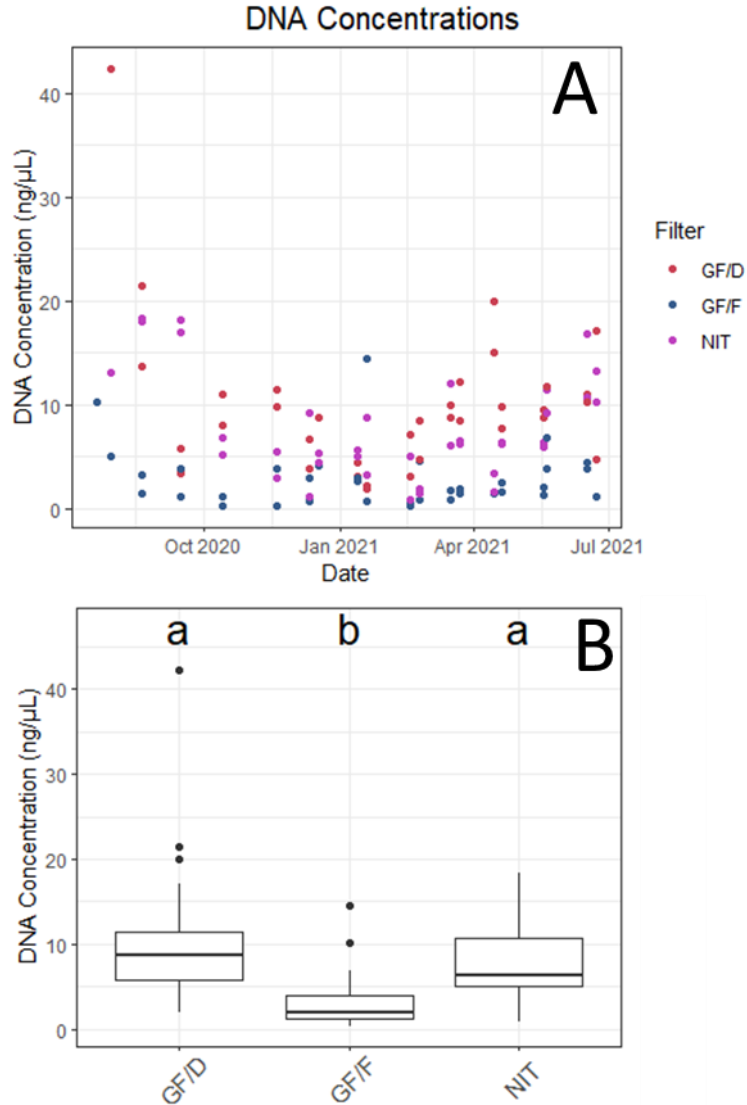


**Figure 6.** Scatterplot (A) and box plot (B) of DNA concentrations from each filter type. One sample (7/21/2020 0 m GF/D) was removed because it had an order of magnitude higher concentration than the other samples and so represented an outlier. Different lowercase letters represent groupings that are significantly different from each other according to Tukey’s HSD test.

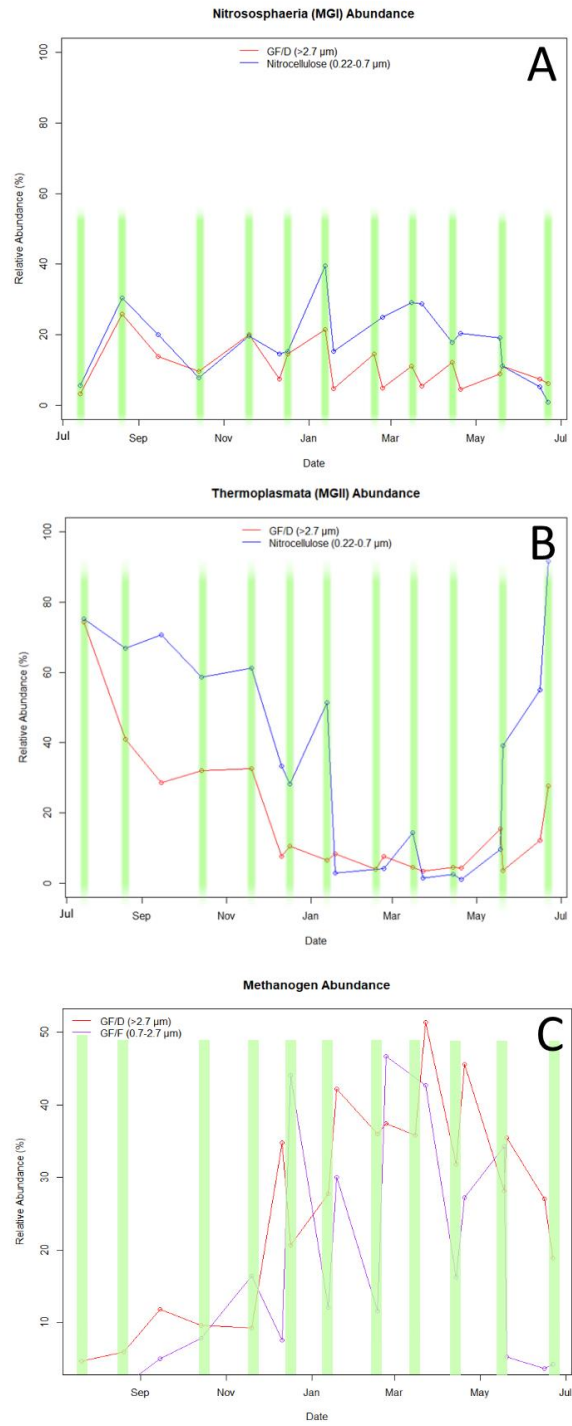


**Figure 7.** Abundance of MGI (A), MGII (B), and total methanogens (C) over time.

Vertical green bars represent samples taken at high tide.

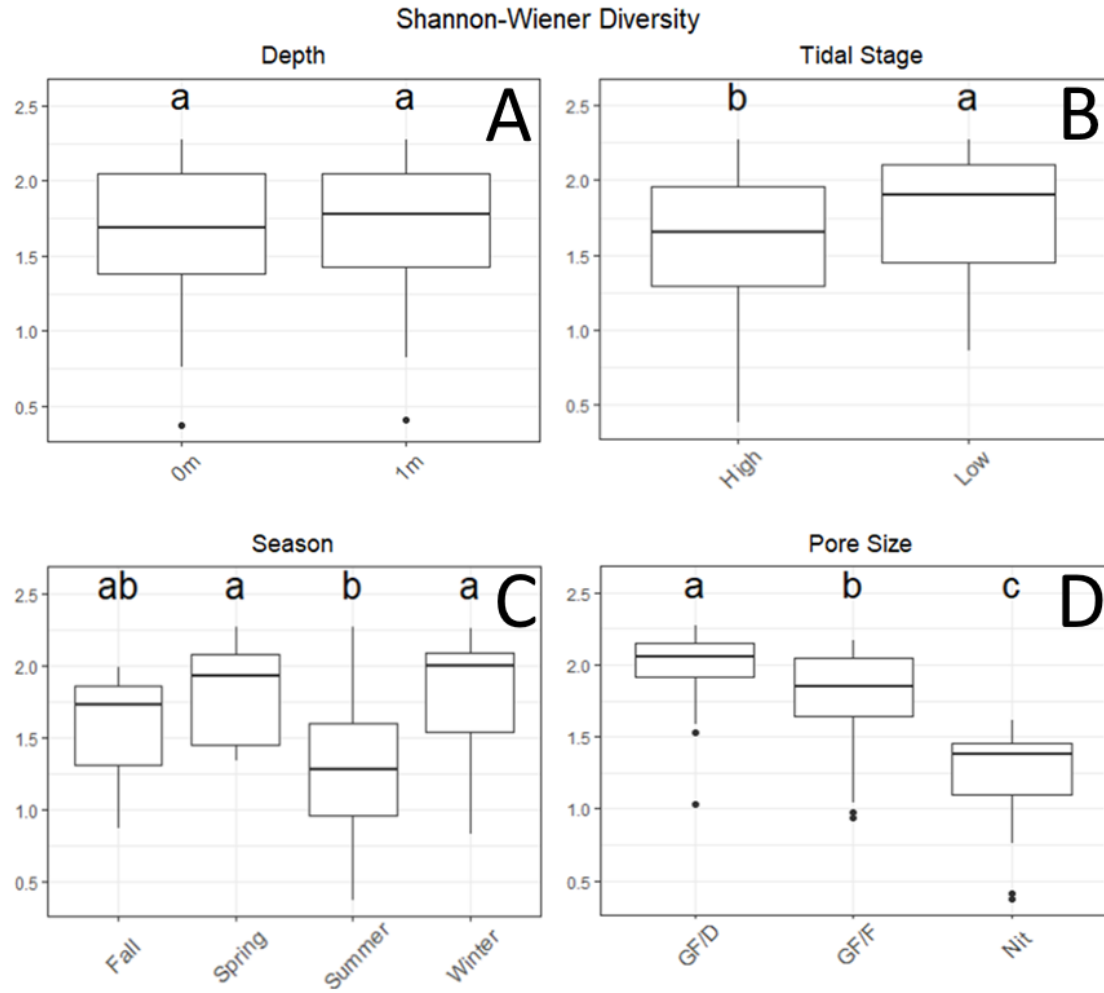


**Figure 8.** Box plots of alpha diversity (Shannon-Wiener index) comparing samples grouped by depth (A), tidal stage (B), season (C), and pore size (D). Different lowercase letters represent groupings that are significantly different from each other according to Tukey's HSD test.

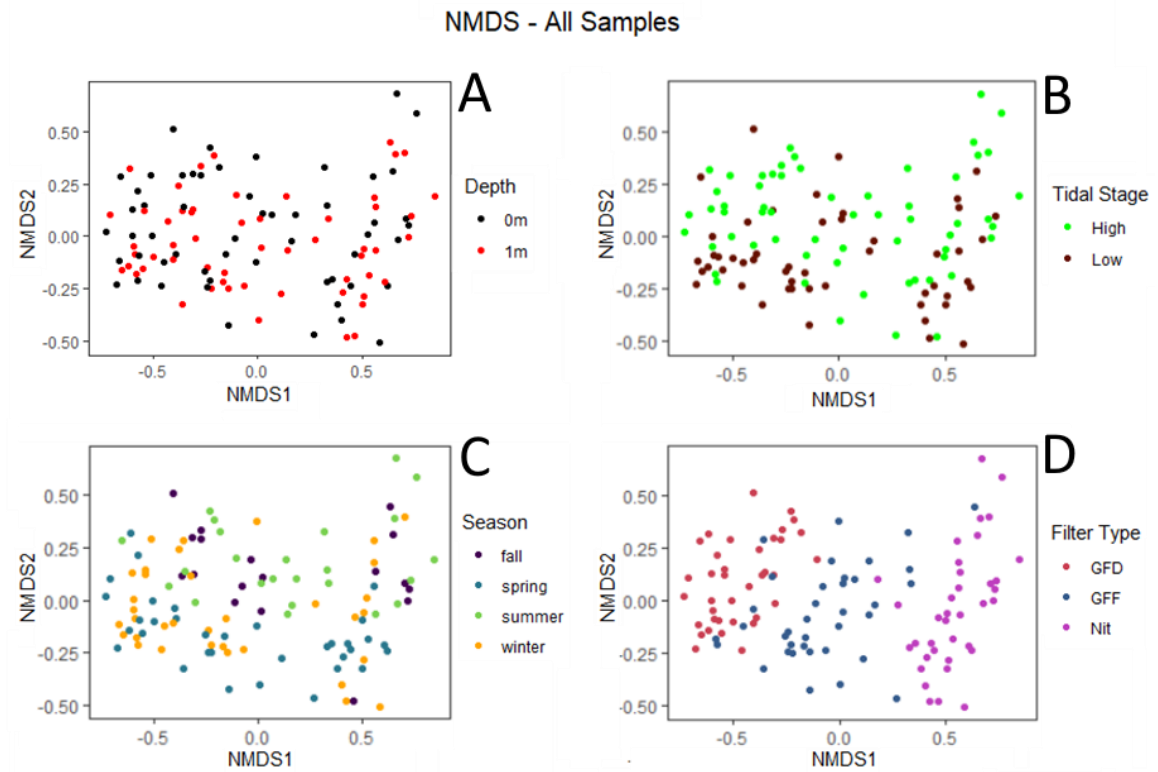


**Figure 9:** NMDS plot of all samples with colors denoting categorical variables: depth (A); tidal stage (B); season (C) and filter type (D) . Data are normalized by scaling with ranked sampling. Stress for the ordination is 0.14.

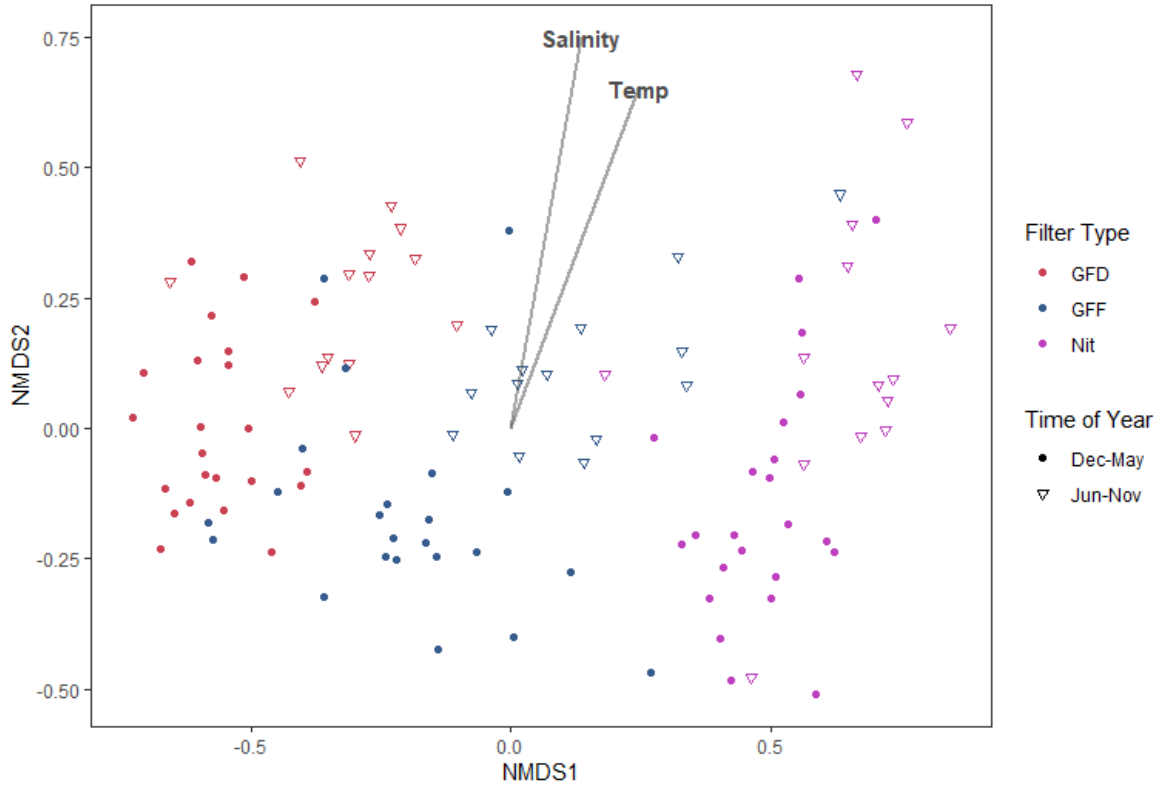


**Figure 10:** NMDS plot of all samples coded by filter type and time of year with pseudo-axes. Lines represent pseudo-axes constructed from environmental variables; the longer the arrow, the greater its predictive value of variation in the community. Stress for the ordination is 0.14.

**Table 1.** Sampling dates and corresponding tidal stages, tide heights, volume filtered, and data from YSI ProSolo probe. Tidal height retrieved from NOAA website (<https://tidesandcurrents.noaa.gov/>) and represents the height approximately halfway through sampling.

Sampling date	Tidal Stage	Tidal Height (meters, MLLW)	Total Volume Filtered (L)		Temperature (°C)		Salinity (PSU)		Dissolved Oxygen (mg/L)		Total Dissolved Solids (mg/L)	
			0m	1m	0m	1m	0m	1m	0m	1m	0m	1m
7/21/2020	High	1.327	16.54	N/A	26.5	N/A	27.42	N/A	6.74	N/A	27760	N/A
7/30/2020	Low	0.211	N/A	16.93	N/A	29.06	N/A	24.91	N/A	3.37	N/A	25524
8/20/2020	High	1.603	17.65	16.15	24.33	24.28	27.43	27.53	7.23	7.2	27727	27822
9/15/2020	Low	0.334	9.15	9.4	21.94	21.89	21.97	22.08	5.32	5.28	22669	22766
10/14/2020	High	1.521	9.55	8.85	18	18.06	27.34	27.35	7.03	6.98	27595	27603
11/19/2020	High	1.558	6.68	7.68	11.94	11.89	27.4	27.45	8.75	8.62	27749	27791
12/11/2020	Low	0.148	6.88	7.03	7.28	7.11	19.56	19.71	9.39	9.42	20588	20744
12/17/2020	High	1.847	4.73	5.28	7.22	7.17	25.32	25.36	9.85	9.79	26063	26095
1/13/2021	High	1.738	13.15	13.98	5.61	5.56	26.84	26.81	10.78	10.78	27612	27588
1/19/2021	Low	0.018	8.8	9.15	4.72	4.67	12.49	12.94	11.36	11.19	13729	14183
2/17/2021	High	1.011	4.08	4.03	2.83	2.78	24.17	24.38	11.68	11.69	25372	25582
2/23/2021	Low	0.272	5.24	6.16	3.22	3.17	15.97	16.05	11.83	11.84	17313	17395
3/16/2021	High	1.474	9.45	10.6	6.56	6.56	26.14	26.21	10.21	10.3	26874	26937
3/23/2021	Low	0.465	8.49	8.39	9.44	9.28	16.64	16.79	9.98	9.96	17678	17822
4/14/2021	High	1.331	7.74	8.79	12.06	11.89	26.21	26.36	8.47	8.6	26650	26791
4/20/2021	Low	0.344	8.04	7.89	13.22	13.17	17.19	17.27	8.25	8.07	18135	18205
5/18/2021	Low	0.142	8.99	9.04	17.28	17.17	22.43	22.6	8.27	8.16	23073	23227
5/20/2021	High	1.087	12.04	12.04	17.89	17.83	28.31	28.38	8.91	9.31	28474	28538
6/16/2021	Low	0.336	9.34	8.29	21.89	21.94	25.49	25.73	6.06	5.97	25921	26142
6/22/2021	High	1.392	11.14	10.79	21.94	21.94	28.6	28.59	6.98	6.83	28758	28741

**Table 2.** Results of linear regressions of Nitrososphaeria (MGI), Thermoplasmata (MGII), and sum of methanogens (Methan.) relative abundance vs. environmental variables and Wilcoxon signed rank test comparing relative abundance in samples taken at high tide vs. samples taken at low tide. Individual linear regressions were performed for each filter type and for all samples combined. Yellow indicates a statistically significant positive correlation (or statistically-significant result for the Wilcoxon test); orange indicates a negative correlation (p-value cutoff 0.05). Methanogen abundance was only analyzed in the larger two size fractions where they were most abundant.

		GF/D			GF/F			Nit		All combined	
		MGI	MGII	Methan.	MGI	MGII	Methan.	MGI	MGII	MGI	MGII
Salinity	p-val	0.000808	0.00672	0.00186	0.112	0.000282	0.0252	0.3123	0.000964	0.088	0.00263
	R <sup>2</sup>	0.2775	0.1917	0.4434	0.07075	0.3175	0.2617	0.02834	0.2642	0.02623	0.2247
ODO	p-val	0.8556	1.63E-05	0.00376	0.8113	0.00113	0.0188	0.00319	0.000434	0.0759	6.68E-09
	R <sup>2</sup>	0.000959	0.4162	0.3983	0.001651	0.2646	0.284	0.2172	0.2943	0.02836	0.2644
Temp	p-val	0.941	1.71E-07	0.00269	0.87289	0.000265	0.00777	0.00232	5.35E-05	0.161	2.18E-11
	R <sup>2</sup>	0.000161	0.5468	0.42	0.000742	0.3198	0.3487	0.2299	0.3684	0.01774	0.3358
TDS	p-val	0.000617	0.009608	0.00231	0.0989	0.000345	0.03032	0.37428	0.0013	0.0669	2.69E-07
	R <sup>2</sup>	0.288	0.1766	0.4298	0.07589	0.31	0.02472	0.02199	0.2527	0.0302	0.2147
Wilcoxon - Tide Comparison	p-val	0.000257	0.3413	0.06916	0.06031	0.03571	0.1602	0.7717	0.05568	0.01826	0.002475

**Table 3.** Results of Indicator Species Analysis test. Shown are the archaeal classes that are more abundant in particular groupings than others (p-value <0.05). Classes in gray are those that do not make up more than 5% of the community in any sample

Poresize				Tidal Stage			
More abundant in...	Class	Stat	p-value	More abundant at...	Class	Stat	p-value
GF/D	Crenarchaeota_unclassified	0.808	0.0001	High Tide	Thermoplasmata	0.306	0.0015
	Methanosarcinia	0.719	0.0001		Lokiarchaeia	0.271	0.0029
	Methanomicrobia	0.712	0.0001		Nitrososphaeria	0.266	0.0045
	Lokiarchaeia	0.513	0.0001	Low Tide	Methanobacteria	0.36	0.0002
	Odinarchaeia	0.487	0.0001		Methanocellia	0.34	0.0002
	Thermoplasmata_cl	0.44	0.0001		Archaea_unclassified	0.277	0.0035
	Thermoplasmata_unclassified	0.438	0.0001		Micrarchaeia	0.205	0.0256
	Halobacterota_unclassified	0.36	0.0001		Nanoarchaeia	0.201	0.032
	Asgardarchaeota_cl	0.338	0.0013		Halobacterota_unclassified	0.196	0.0279
	Methanomethylica	0.323	0.0012		Methanomethylica	0.193	0.0389
Thermococci	0.304	0.0001					
Thermoprotei	0.226	0.0251					
Depth				Season			
More abundant at...	Class	Stat	p-value	More abundant in...	Class	Stat	p-value
Nitrocellulose	Nanoarchaeia	0.597	0.0001	Spring	Archaea_unclassified	0.449	0.0001
	Aenigmarchaeota_unclassified	0.444	0.0001		unknown_unclassified	0.387	0.0001
	Thermoplasmata	0.326	0.0012		Nanoarchaeia	0.301	0.015
GF/D + GF/F	Deep_Sea_Euryarchaeotic_Group	0.285	0.0053	Winter	Halobacterota_unclassified	0.296	0.0116
	Methanocellia	0.54	0.0001		Micrarchaeia	0.259	0.0403
	Methanobacteria	0.519	0.0001	Fall + Summer	Thermoplasmata	0.689	1.00E-04
Euryarchaeota_unclassified	0.337	0.0014	Spring + Winter		Methanocellia	0.462	0.0001
GF/F + Nitrocellulose	Archaea_unclassified	0.397		0.0002	Methanobacteria	0.458	0.0002
	Nitrososphaeria	0.326		0.0014	Methanomicrobia	0.422	0.0002
	unknown_unclassified	0.229		0.0231	Methanosarcinia	0.357	0.0024
0m	Thermoprotei	0.166		0.0478	Euryarchaeota_unclassified	0.294	0.0144

**Table 4.** Results of ANOSIM (Analysis of Similarities) test comparing the community structure between different groupings. Yellow cells indicate a significant p-value (<0.05).

“Yearsplit” indicates Dec-May vs. Jun-Nov.

	Pore size	GF/D vs GF/F	GF/D vs Nit	GF/F vs Nit	Depth	Tide	Season	Yearsplit
<b>ANOSIM statistic R</b>	0.452	0.3299	0.7219	0.3299	-0.01607	0.08863	0.2399	0.3083
<b>Significance</b>	1.00E-04	1.00E-04	1.00E-04	1.00E-04	0.9876	7.00E-04	1.00E-04	1.00E-04

**Table 5.** Results of Mantel test comparing Euclidean distance vectors constructed from environmental variables with a Bray-Curtis dissimilarity matrix of all samples.

Highlighted cells indicate significant p-values.

	<b>Temperature</b>	<b>Salinity</b>	<b>ODO</b>	<b>TDS</b>
<b>Mantel statistic r</b>	0.1857	0.1787	0.107	0.1772
<b>Significance</b>	1.00E-04	1.00E-04	3.00E-04	1.00E-04

## REFERENCES

- Adam, P. S., Borrel, G., Brochier-Armanet, C., & Gribaldo, S. (2017). The growing tree of Archaea: new perspectives on their diversity, evolution and ecology. *The ISME Journal* 2017 11:11, 11(11), 2407–2425. <https://doi.org/10.1038/ismej.2017.122>
- Anas, A., Balu, B. T., Jasmin, C., Chandran, C., Vipindas, P. V., Narayanan, S., & Abdul, A. J. (2021). Microbial community shifts along an estuarine to open ocean continuum. *Regional Studies in Marine Science*, 41, 101587. <https://doi.org/10.1016/J.RSMA.2020.101587>
- Anderson, I., Ulrich, L. E., Lupa, B., Susanti, D., Porat, I., Hooper, S. D., Lykidis, A., Sieprawska-Lupa, M., Dharmarajan, L., Goltsman, E., Lapidus, A., Saunders, E., Han, C., Land, M., Lucas, S., Mukhopadhyay, B., Whitman, W. B., Woese, C., Bristow, J., & Kyrpides, N. (2009). Genomic Characterization of Methanomicrobiales Reveals Three Classes of Methanogens. *PLOS ONE*, 4(6), e5797. <https://doi.org/10.1371/JOURNAL.PONE.0005797>
- Anderson, B. G., Bell, M. L., & Peng, R. D. (2013). Methods to calculate the heat index as an exposure metric in environmental health research. *Environmental Health Perspectives*, 121(10), 1111–1119. <https://doi.org/10.1289/EHP.1206273>
- Andrews, S. (2010). FastQC: A Quality Control Tool for High Throughput Sequence Data [Online]. Available online at: <http://www.bioinformatics.babraham.ac.uk/projects/fastqc/>
- Angle, J. C., Morin, T. H., Solden, L. M., Narrowe, A. B., Smith, G. J., Borton, M. A., Rey-Sanchez, C., Daly, R. A., Mirfenderesgi, G., Hoyt, D. W., Riley, W. J., Miller, C. S., Bohrer, G., & Wrighton, K. C. (2017). Methanogenesis in oxygenated soils is a substantial fraction of wetland methane emissions. *Nature Communications* 2017 8:1, 8(1), 1–9. <https://doi.org/10.1038/s41467-017-01753-4>

- Auguie, Baptiste (2017). gridExtra: Miscellaneous Functions for "Grid" Graphics. R package version 2.3. <https://CRAN.R-project.org/package=gridExtra>
- Baltar, F., Arístegui, J., Gasol, J. M., Hernández-León, S., & Herndl, G. J. (2007). Strong coast–ocean and surface–depth gradients in prokaryotic assemblage structure and activity in a coastal transition zone region. *Aquatic Microbial Ecology*, *50*(1), 63–74. <https://doi.org/10.3354/AME01156>
- Bange, H. W., Bartell, U. H., Rapsomanikis, S., & Andreae, M. O. (1994). Methane in the Baltic and North Seas and a reassessment of the marine emissions of methane. *Global Biogeochemical Cycles*, *8*(4), 465–480. <https://doi.org/10.1029/94GB02181>
- Baumgartner, L. K., Spear, J. R., Buckley, D. H., Pace, N. R., Reid, R. P., Dupraz, C., & Visscher, P. T. (2009). Microbial diversity in modern marine stromatolites, Highborne Cay, Bahamas. *Environmental Microbiology*, *11*(10), 2710–2719. <https://doi.org/10.1111/J.1462-2920.2009.01998.X>
- Beman, J. M., Steele, J. A., & Fuhrman, J. A. (2011). Co-occurrence patterns for abundant marine archaeal and bacterial lineages in the deep chlorophyll maximum of coastal California. *The ISME Journal* *2011* 5:7, *5*(7), 1077–1085. <https://doi.org/10.1038/ISMEJ.2010.204>
- Besseling, M. A., Hopmans, E. C., Bale, N. J., Schouten, S., Damsté, J. S. S., & Villanueva, L. (2020). The absence of intact polar lipid-derived GDGTs in marine waters dominated by Marine Group II: Implications for lipid biosynthesis in Archaea. *Scientific Reports*, *10*(1), 1–10. <https://doi.org/10.1038/s41598-019-57035-0>
- Beule, L., & Karlovsky, P. (2020). Improved normalization of species count data in ecology by scaling with ranked subsampling (SRS): Application to microbial communities. *PeerJ*, *8*, e9593. <https://doi.org/10.7717/PEERJ.9593/SUPP-2>

- Biddle, J. F., Lipp, J. S., Lever, M. A., Lloyd, K. G., Sørensen, K. B., Anderson, R., Fredricks, H. F., Elvert, M., Kelly, T. J., Schrag, D. P., Sogin, M. L., Brenchley, J. E., Teske, A., House, C. H., & Hinrichs, K. U. (2006). Heterotrophic Archaea dominate sedimentary subsurface ecosystems off Peru. *Proceedings of the National Academy of Sciences of the United States of America*, *103*(10), 3846–3851. [https://doi.org/10.1073/PNAS.0600035103/SUPPL\\_FILE/00035FIG4.PDF](https://doi.org/10.1073/PNAS.0600035103/SUPPL_FILE/00035FIG4.PDF)
- Bligh, E. G., & Dyer, W. J. (1959). A RAPID METHOD OF TOTAL LIPID EXTRACTION AND PURIFICATION. *Canadian Journal of Biochemistry and Physiology*, *37*(8), 911–917. <https://doi.org/https://doi.org/10.1139/o59-099>
- Bogard, M. J., Del Giorgio, P. A., Boutet, L., Chaves, M. C. G., Prairie, Y. T., Merante, A., & Derry, A. M. (2014). Oxic water column methanogenesis as a major component of aquatic CH<sub>4</sub> fluxes. *Nature Communications 2014 5:1*, *5*(1), 1–9. <https://doi.org/10.1038/ncomms6350>
- Bonin, A. S., & Boone, D. R. (2006). The Order Methanobacteriales. In M. Dworkin, S. Falkow, E. Rosenberg, K.-H. Schleifer, & E. Stackebrandt (Eds.), *The Prokaryotes* (3rd ed., Vol. 3, pp. 231–243). Springer. [https://doi.org/10.1007/0-387-30743-5\\_11](https://doi.org/10.1007/0-387-30743-5_11)
- Brochier-Armanet, C., Boussau, B., Gribaldo, S., & Forterre, P. (2008). Mesophilic crenarchaeota: proposal for a third archaeal phylum, the Thaumarchaeota. *Nature Reviews Microbiology*, *6*(3), 245–252. <https://doi.org/10.1038/nrmicro1852>
- Buan, N. R. (2018). Methanogens: pushing the boundaries of biology. *Emerging Topics in Life Sciences*, *2*(4), 629. <https://doi.org/10.1042/ETLS20180031>
- Bulzu, P. A., Andrei, A. Ş., Salcher, M. M., Mehrshad, M., Inoue, K., Kandori, H., Beja, O., Ghai, R., & Banciu, H. L. (2019). Casting light on Asgardarchaeota metabolism in a sunlit microoxic niche. *Nature Microbiology 2019 4:7*, *4*(7), 1129–1137. <https://doi.org/10.1038/s41564-019-0404-y>

- Campbell, B. J., & Kirchman, D. L. (2013). Bacterial diversity, community structure and potential growth rates along an estuarine salinity gradient. *The ISME Journal* 2013 7:1, 7(1), 210–220. <https://doi.org/10.1038/ismej.2012.93>
- Castelle, C. J., Wrighton, K. C., Thomas, B. C., Hug, L. A., Brown, C. T., Wilkins, M. J., Frischkorn, K. R., Tringe, S. G., Singh, A., Markillie, L. M., Taylor, R. C., Williams, K. H., & Banfield, J. F. (2015). Genomic Expansion of Domain Archaea Highlights Roles for Organisms from New Phyla in Anaerobic Carbon Cycling. *Current Biology*, 25(6), 690–701. <https://doi.org/10.1016/J.CUB.2015.01.014>
- Chen, S., Wang, P., Liu, H., Xie, W., Wan, X. S., Kao, S. J., Phelps, T. J., & Zhang, C. (2019). Population dynamics of methanogens and methanotrophs along the salinity gradient in Pearl River Estuary: implications for methane metabolism. *Applied Microbiology and Biotechnology* 2019 104:3, 104(3), 1331–1346. <https://doi.org/10.1007/S00253-019-10221-6>
- Church, M. J., DeLong, E. F., Ducklow, H. W., Karner, M. B., Preston, C. M., & Karl, D. M. (2003). Abundance and distribution of planktonic Archaea and Bacteria in the waters west of the Antarctic Peninsula. *Limnology and Oceanography*, 48(5), 1893–1902. <https://doi.org/10.4319/lo.2003.48.5.1893>
- Ciulla, R., Clougherty, C., Belay, N., Krishnan, S., Zhou, C., Byrd, D., & Roberts, M. F. (1994). Halotolerance of *Methanobacterium thermoautotrophicum* delta H and Marburg. *Journal of Bacteriology*, 176(11), 3177. <https://doi.org/10.1128/JB.176.11.3177-3187.1994>
- Close, H. G., Shah, S. R., Ingalls, A. E., Diefendorf, A. F., Brodie, E. L., Hansman, R. L., Freeman, K. H., Aluwihare, L. I., & Pearson, A. (2013). Export of submicron particulate organic matter to mesopelagic depth in an oligotrophic gyre. *Proceedings of the National Academy of Sciences of the United States of America*, 110(31),

12565–12570.

[https://doi.org/10.1073/PNAS.1217514110/SUPPL\\_FILE/PNAS.201217514SI.PDF](https://doi.org/10.1073/PNAS.1217514110/SUPPL_FILE/PNAS.201217514SI.PDF)

- Crump, B. C., & Baross, J. A. (1996). Particle-attached bacteria and heterotrophic plankton associated with the Columbia River estuarine turbidity maxima. *Marine Ecology Progress Series*, 138(1–3), 265–273. <https://doi.org/10.3354/meps138265>
- Crump, B. C., Baross, J. A., & Simenstad, C. A. (1998). Dominance of particle-attached bacteria in the Columbia River estuary, USA. *Aquatic Microbial Ecology*, 14(1), 7–18. <https://doi.org/10.3354/AME014007>
- Crump, B. C., Armbrust, E. V., & Baross, J. A. (1999). Phylogenetic analysis of particle-attached and free-living bacterial communities in the Columbia river, its estuary, and the adjacent coastal ocean. *Applied and Environmental Microbiology*, 65(7), 3192–3204. <https://doi.org/10.1128/AEM.65.7.3192-3204.1999>
- Damm, E., Helmke, E., Thoms, S., Schauer, U., Nöthig, E., Bakker, K., & Kiene, R. P. (2010). Methane production in aerobic oligotrophic surface water in the central Arctic Ocean. *Biogeosciences*, 7(3), 1099–1108. <https://doi.org/10.5194/BG-7-1099-2010>
- Dexter, E., Rollwagen-Bollens, G., & Bollens, S. M. (2018). The trouble with stress: A flexible method for the evaluation of nonmetric multidimensional scaling. *Limnology and Oceanography: Methods*, 16(7), 434–443. <https://doi.org/10.1002/LOM3.10257>
- DNREC, Delaware Sea Grant, U. of D. (2022). *Delaware Water Quality Portal*. <http://demac.udel.edu/waterquality/about.php>
- DeLong, E. F. (1992). Archaea in coastal marine environments. *Proceedings of the National Academy of Sciences*, 89(12), 5685–5689. <https://doi.org/10.1073/pnas.89.12.5685>

- DeLong, E. F. (2021). Exploring Marine Planktonic Archaea: Then and Now. *Frontiers in Microbiology*, *11*, 3527. <https://doi.org/10.3389/FMICB.2020.616086/BIBTEX>
- Denman, S. E., & McSweeney, C. S. (2006). Development of a real-time PCR assay for monitoring anaerobic fungal and cellulolytic bacterial populations within the rumen. *FEMS Microbiology Ecology*, *58*(3), 572–582. <https://doi.org/10.1111/J.1574-6941.2006.00190.X>
- Dewitt, P., & Daiber, F. C. (1973). The hydrography of the Broadkill River estuary, Delaware. *Chesapeake Science*, *14*(1), 28–40. <https://doi.org/10.2307/1350700>
- De Cáceres, M., Legendre, P., Moretti, M., De Cáceres, M., Legendre, P., & Moretti, M. (2010). Improving indicator species analysis by combining groups of sites. *Oikos*, *119*(10), 1674–1684. <https://doi.org/10.1111/J.1600-0706.2010.18334.X>
- de Mendiburu, Felipe (2021). agricolae: Statistical Procedures for Agricultural Research. R package version 1.3-5. <https://CRAN.R-project.org/package=agricolae>
- Ferry, J. G., & Lessner, D. J. (2008). Methanogenesis in Marine Sediments. *Annals of the New York Academy of Sciences*, *1125*(1), 147–157. <https://doi.org/10.1196/ANNALS.1419.007>
- Francis, C. A., Roberts, K. J., Beman, J. M., Santoro, A. E., & Oakley, B. B. (2005). Ubiquity and diversity of ammonia-oxidizing archaea in water columns and sediments of the ocean. *Proceedings of the National Academy of Sciences of the United States of America*, *102*(41), 14683–14688. <https://doi.org/10.1073/PNAS.0506625102>
- Frigaard, N. U., Martinez, A., Mincer, T. J., & DeLong, E. F. (2006). Proteorhodopsin lateral gene transfer between marine planktonic Bacteria and Archaea. *Nature*, *439*(7078), 847–850. <https://doi.org/10.1038/nature04435>

- Fuhrman, J. A., Hewson, I., Schwalbach, M. S., Steele, J. A., Brown, M. V., & Naeem, S. (2006). Annually reoccurring bacterial communities are predictable from ocean conditions. *Proceedings of the National Academy of Sciences of the United States of America*, *103*(35), 13104–13109. <https://doi.org/10.1073/PNAS.0602399103>
- Galand, P. E., Gutiérrez-Provecho, C., Massana, R., Gasol, J. M., & Casamayor, E. O. (2010). Inter-annual recurrence of archaeal assemblages in the coastal NW Mediterranean Sea (Blanes Bay Microbial Observatory). *Limnology and Oceanography*, *55*(5), 2117–2125. <https://doi.org/10.4319/lo.2010.55.5.2117>
- Garcia, J.-L., Ollivier, B., & Whitman, W. B. (2006). The Order Methanomicrobiales. In M. Dworkin, S. Falkow, E. Rosenberg, K.-H. Schleifer, & E. Stackebrandt (Eds.), *The Prokaryotes* (3rd ed., pp. 208–230). Springer. [https://doi.org/10.1007/0-387-3074305\\_10](https://doi.org/10.1007/0-387-3074305_10)
- Garnier Simon, Noam Ross, Robert Rudis, Antônio P. Camargo, Marco Sciaini, and Cédric Scherer (2021). Rvision - Colorblind-Friendly Color Maps for R. R package version 0.6.2.
- Gilbert, J. A., Steele, J. A., Caporaso, J. G., Steinbrück, L., Reeder, J., Temperton, B., Huse, S., McHardy, A. C., Knight, R., Joint, I., Somerfield, P., Fuhrman, J. A., & Field, D. (2011). Defining seasonal marine microbial community dynamics. *The ISME Journal* *2012* 6:2, 6(2), 298–308. <https://doi.org/10.1038/ismej.2011.107>
- Guadayol, Ò., Peters, F., Marrasé, C., Gasol, J. M., Roldán, C., Berdalet, E., Massana, R., & Sabata, A. (2009). Episodic meteorological and nutrient-load events as drivers of coastal planktonic ecosystem dynamics: a time-series analysis. *Marine Ecology Progress Series*, *381*, 139–155. <https://doi.org/10.3354/MEPS07939>
- Hao, D. M., Tashiro, T., Kato, M., Sohrin, R., Ishibashi, T., Katsuyama, C., Nagaosa, K., Kimura, H., Thanh, T. D., & Kato, K. (2010). Population Dynamics of

- Crenarchaeota and Euryarchaeota in the Mixing Front of River and Marine Waters. *Microbes and Environments*, 25(2), 126–132.  
<https://doi.org/10.1264/JSME2.ME10106>
- Herfort, L., Schouten, S., Abbas, B., Veldhuis, M. J. W., Coolen, M. J. L., Wuchter, C., Boon, J. P., Herndl, G. J., & Sinninghe Damsté, J. S. (2007). Variations in spatial and temporal distribution of Archaea in the North Sea in relation to environmental variables. *FEMS Microbiology Ecology*, 62(3), 242–257.  
<https://doi.org/10.1111/J.1574-6941.2007.00397.X>
- Huber, H., Hohn, M. J., Rachel, R., Fuchs, T., Wimmer, V. C., & Stetter, K. O. (2002). A new phylum of Archaea represented by a nanosized hyperthermophilic symbiont. *Nature*, 417(6884), 63–67. <https://doi.org/10.1038/417063A>
- Hugoni, M., Taib, N., Debros, D., Domaizon, I., Dufournel, I. J., Bronner, G., Salter, I., Agogué, H., Mary, I., & Galand, P. E. (2013). Structure of the rare archaeal biosphere and seasonal dynamics of active ecotypes in surface coastal waters. *Proceedings of the National Academy of Sciences of the United States of America*, 110(15), 6004–6009. <https://doi.org/10.1073/pnas.1216863110>
- Huot, Y., Babin, M., Bruyant, F., Grob, C., Twardowski, M. S., & Claustre, H. (2007). Does chlorophyll a provide the best index of phytoplankton biomass for primary productivity studies? *Biogeosciences Discussions*, 4(2), 707–745.  
<https://doi.org/10.5194/BGD-4-707-2007>
- Hurley, S. J., Lipp, J. S., Close, H. G., Hinrichs, K. U., & Pearson, A. (2018). Distribution and export of isoprenoid tetraether lipids in suspended particulate matter from the water column of the Western Atlantic Ocean. *Organic Geochemistry*, 116, 90–102. <https://doi.org/10.1016/j.orggeochem.2017.11.010>

- Ingalls, A. E., Shah, S. R., Hansman, R. L., Aluwihare, L. I., Santos, G. M., Druffel, E. R. M., & Pearson, A. (2006). Quantifying archaeal community autotrophy in the mesopelagic ocean using natural radiocarbon. *Proceedings of the National Academy of Sciences*, *103*(17), 6442–6447. <https://doi.org/10.1073/pnas.0510157103>
- Iverson, V., Morris, R. M., Frazar, C. D., Berthiaume, C. T., Morales, R. L., & Armbrust, E. V. (2012). Untangling genomes from metagenomes: Revealing an uncultured class of marine euryarchaeota. *Science*, *335*(6068), 587–590. <https://doi.org/10.1126/science.1212665>
- Jain, A., & Krishnan, K. P. (2021). Marine Group-II archaea dominate particle-attached as well as free-living archaeal assemblages in the surface waters of Kongsfjorden, Svalbard, Arctic Ocean. *Antonie van Leeuwenhoek, International Journal of General and Molecular Microbiology*, *114*(5), 633–647. <https://doi.org/10.1007/S10482-021-01547-1/>
- Jarett, J. K., Nayfach, S., Podar, M., Inskeep, W., Ivanova, N. N., Munson-Mcgee, J., Schulz, F., Young, M., Jay, Z. J., Beam, J. P., Kyrpides, N. C., Malmstrom, R. R., Stepanauskas, R., & Woyke, T. (2018). Single-cell genomics of co-sorted Nanoarchaeota suggests novel putative host associations and diversification of proteins involved in symbiosis 06 Biological Sciences 0604 Genetics. *Microbiome*, *6*(1), 1–14. <https://doi.org/10.1186/S40168-018-0539-8>
- Kassambara, Alboukadel (2020). ggpubr: 'ggplot2' Based Publication Ready Plots. R package version 0.4.0. <https://CRAN.R-project.org/package=ggpubr>
- Kellogg, C. T. E., & Deming, J. W. (2009). Comparison of free-living, suspended particle, and aggregate-associated bacterial and archaeal communities in the Laptev Sea. *Aquatic Microbial Ecology*, *57*(1), 1–18. <https://doi.org/10.3354/AME01317>

- Kendall, M. M., & Boone, D. R. (2006). The Order Methanosarcinales. In M. Dworkin, S. Falkow, E. Rosenberg, K.-H. Schleifer, & E. Stackebrandt (Eds.), *The Prokaryotes* (3rd ed., Vol. 3, pp. 244–256). Springer. [https://doi.org/10.1007/0-387-30743-5\\_12](https://doi.org/10.1007/0-387-30743-5_12)
- Könneke, M., Bernhard, A. E., de la Torre, J. R., Walker, C. B., Waterbury, J. B., & Stahl, D. A. (2005). Isolation of an autotrophic ammonia-oxidizing marine archaeon. *Nature*, *437*(7058), 543–546. <https://doi.org/10.1038/nature03911>
- Könneke, M., Schubert, D. M., Brown, P. C., Hügler, M., Standfest, S., Schwander, T., Schada von Borzyskowski, L., Erb, T. J., Stahl, D. A., & Berg, I. A. (2014). Ammonia-oxidizing archaea use the most energy-efficient aerobic pathway for CO<sub>2</sub> fixation. *Proceedings of the National Academy of Sciences of the United States of America*, *111*(22), 8239–8244. <https://doi.org/10.1073/pnas.1402028111>
- Lange, V., Böhme, I., Hofmann, J., Lang, K., Sauter, J., Schöne, B., Paul, P., Albrecht, V., Andreas, J. M., Baier, D. M., Nething, J., Ehninger, U., Schwarzelt, C., Pingel, J., Ehninger, G., & Schmidt, A. H. (2014). Cost-efficient high-throughput HLA typing by MiSeq amplicon sequencing. *BMC Genomics*, *15*(1), 1–11. <https://doi.org/10.1186/1471-2164-15-63>
- Lazar, C. S., Baker, B. J., Seitz, K., Hyde, A. S., Dick, G. J., Hinrichs, K. U., & Teske, A. P. (2016). Genomic evidence for distinct carbon substrate preferences and ecological niches of Bathyarchaeota in estuarine sediments. *Environmental Microbiology*, *18*(4), 1200–1211. <https://doi.org/10.1111/1462-2920.13142>
- Leonte, M., Ruppel, C. D., Ruiz-Angulo, A., & Kessler, J. D. (2020). Surface Methane Concentrations Along the Mid-Atlantic Bight Driven by Aerobic Subsurface Production Rather Than Seafloor Gas Seeps. *Journal of Geophysical Research: Oceans*, *125*(5), e2019JC015989. <https://doi.org/10.1029/2019JC015989>

- Levipan, H. A., Quiñones, R. A., Johansson, H. E., & Urrutia, H. (2007). Methylophilic Methanogens in the Water Column of an Upwelling Zone with a Strong Oxygen Gradient Off Central Chile. *Microbes and Environments*, 22(3), 268–278. <https://doi.org/10.1264/JSME2.22.268>
- Lincoln, S. A., Wai, B., Eppley, J. M., Church, M. J., Summons, R. E., & DeLong, E. F. (2014). Planktonic Euryarchaeota are a significant source of archaeal tetraether lipids in the ocean. *Proceedings of the National Academy of Sciences of the United States of America*, 111(27), 9858–9863. <https://doi.org/10.1073/pnas.1409439111>
- Lincoln, S. A., Wai, B., Eppley, J. M., Church, M. J., Summons, R. E., & DeLong, E. F. (2014). Reply to Schouten et al.: Marine Group II planktonic Euryarchaeota are significant contributors to tetraether lipids in the ocean. *Proceedings of the National Academy of Sciences of the United States of America*, 111(41), E4286. <https://doi.org/10.1073/pnas.1416736111>
- Liu, J., Yu, S., Zhao, M., He, B., & Zhang, X. H. (2014). Shifts in archaeoplankton community structure along ecological gradients of Pearl Estuary. *FEMS Microbiology Ecology*, 90(2), 424–435. <https://doi.org/10.1111/1574-6941.12404/-/DC1>
- Liu, X., Pan, J., Liu, Y., Li, M., & Gu, J. D. (2018). Diversity and distribution of Archaea in global estuarine ecosystems. *Science of The Total Environment*, 637–638, 349–358. <https://doi.org/10.1016/J.SCITOTENV.2018.05.016>
- Lyu, Z., Shao, N., Akinyemi, T., & Whitman, W. B. (2018). Methanogenesis. *Current Biology*, 28(13), R727–R732. <https://doi.org/10.1016/J.CUB.2018.05.021>
- Ma, C., Coffinet, S., Lipp, J. S., Hinrichs, K. U., & Zhang, C. (2020). Marine Group II Euryarchaeota Contribute to the Archaeal Lipid Pool in Northwestern Pacific Ocean

- Surface Waters. *Frontiers in Microbiology*, *11*, 1034.  
<https://doi.org/10.3389/fmicb.2020.01034>
- Mahto, Ananda (2019). splitstackshape: Stack and Reshape Datasets After Splitting Concatenated Values. R package version 1.4.8. <https://CRAN.R-project.org/package=splitstackshape>
- Massana, R., Delong, E. F., & Pedrós-Alió, C. (2000). A few cosmopolitan phylotypes dominate planktonic archaeal assemblages in widely different oceanic provinces. *Applied and Environmental Microbiology*, *66*(5), 1777–1787.  
<https://doi.org/10.1128/AEM.66.5.1777-1787.2000/ASSET/7473ED29-AEB1-4FB8-B17D-248476BDACE9/ASSETS/GRAPHIC/AM0501574005.JPEG>
- McMurdie, P. J., & Holmes, S. (2014). Waste Not, Want Not: Why Rarefying Microbiome Data Is Inadmissible. *PLOS Computational Biology*, *10*(4), e1003531.  
<https://doi.org/10.1371/JOURNAL.PCBI.1003531>
- Mestre, M., Ruiz-González, C., Logares, R., Duarte, C. M., Gasol, J. M., & Sala, M. M. (2018). Sinking particles promote vertical connectivity in the ocean microbiome. *Proceedings of the National Academy of Sciences of the United States of America*, *115*(29), E6799–E6807.  
[https://doi.org/10.1073/PNAS.1802470115/SUPPL\\_FILE/PNAS.1802470115.SAPP.PDF](https://doi.org/10.1073/PNAS.1802470115/SUPPL_FILE/PNAS.1802470115.SAPP.PDF)
- Molina, V., Belmar, L., Levipan, H. A., Ramírez-Flandes, S., Anguita, C., Galán, A., Montes, I., & Ulloa, O. (2020). Spatiotemporal Distribution of Key Pelagic Microbes in a Seasonal Oxygen-Deficient Coastal Upwelling System of the Eastern South Pacific Ocean. *Frontiers in Marine Science*, *7*, 795.  
<https://doi.org/10.3389/FMARS.2020.561597/BIBTEX>

- Murray, A. E., Blakis, A., Massana, R., Strawzewski, S., Passow, U., Alldredge, A., & DeLong, E. F. (1999). A time series assessment of planktonic archaeal variability in the Santa Barbara Channel. *Aquatic Microbial Ecology*, 20(2), 129–145. <https://doi.org/10.3354/AME020129>
- Needham, D. M., & Fuhrman, J. A. (2016). Pronounced daily succession of phytoplankton, archaea and bacteria following a spring bloom. *Nature Microbiology*, 1, 16005. <https://doi.org/10.1038/NMICROBIOL.2016.5>
- Offre, P., Spang, A., & Schleper, C. (2013). Archaea in Biogeochemical Cycles. *Annual Review of Microbiology*, 67(1), 437–457. <https://doi.org/10.1146/annurev-micro-092412-155614>
- Oksanen, J., Blanchet, F. G., Friendly, M., Kindt, R., Legendre, P., McGlinn, D., Minchin, P. R., O’Hara, R. b., Simpson, G. L., Solymos, P., Stevens, M. H. H., Szoecs, E., & Wagner, H. (2019). *Vegan: community ecology package | McGlinn lab*. [https://www.mcglinnlab.org/publication/2019-01-01\\_oxsanen\\_vegan\\_2019/](https://www.mcglinnlab.org/publication/2019-01-01_oxsanen_vegan_2019/)
- Orellana, L. H., Ben Francis, T., Krüger, K., Teeling, H., Müller, M. C., Fuchs, B. M., Konstantinidis, K. T., & Amann, R. I. (2019). Niche differentiation among annually recurrent coastal Marine Group II Euryarchaeota. *The ISME Journal* 2019 13:12, 13(12), 3024–3036. <https://doi.org/10.1038/s41396-019-0491-z>
- Orsi, W. D., Smith, J. M., Wilcox, H. M., Swalwell, J. E., Carini, P., Worden, A. Z., & Santoro, A. E. (2015). Ecophysiology of uncultivated marine euryarchaea is linked to particulate organic matter. *ISME Journal*, 9(8), 1747–1763. <https://doi.org/10.1038/ismej.2014.260>
- Ou, Jianhong (2021). colorBlindness: Safe Color Set for Color Blindness. R package version 0.1.9. <https://CRAN.R-project.org/package=colorBlindness>

- Ouverney, C. C., & Fuhrman, J. A. (2000). Marine planktonic archaea take up amino acids. *Applied and Environmental Microbiology*, *66*(11), 4829–4833. <https://doi.org/10.1128/AEM.66.11.4829-4833.2000>
- Pernthaler, A., Preston, C. M., Pernthaler, J., DeLong, E. F., & Amann, R. (2002). Comparison of fluorescently labeled oligonucleotide and polynucleotide probes for the detection of pelagic marine bacteria and archaea. *Applied and Environmental Microbiology*, *68*(2), 661–667. <https://doi.org/10.1128/AEM.68.2.661-667.2002>
- Pester, M., Schleper, C., & Wagner, M. (2011). The Thaumarchaeota: an emerging view of their phylogeny and ecophysiology. *Current Opinion in Microbiology*, *14*(3), 300–306. <https://doi.org/10.1016/j.mib.2011.04.007>
- Quaiser, A., Zivanovic, Y., Moreira, D., & López-García, P. (2011). Comparative metagenomics of bathypelagic plankton and bottom sediment from the Sea of Marmara. *The ISME Journal*, *5*(2), 285–304. <https://doi.org/10.1038/ISMEJ.2010.113>
- Quast, C., Pruesse, E., Yilmaz, P., Gerken, J., Schweer, T., Yarza, P., Peplies, J., & Glöckner, F. O. (2013). The SILVA ribosomal RNA gene database project: improved data processing and web-based tools. *Nucleic Acids Research*, *41*(D1), D590–D596. <https://doi.org/10.1093/NAR/GKS1219>
- Quiñones, R. A., Levipan, H. A., & González, R. R. (2009). Spatial and temporal variability of planktonic archaeal abundance in the Humboldt Current System off Chile. *Deep Sea Research Part II: Topical Studies in Oceanography*, *56*(16), 1073–1082. <https://doi.org/10.1016/J.DSR2.2008.09.012>
- Ramette, A. (2007). Multivariate analyses in microbial ecology. *FEMS Microbiology Ecology*, *62*(2), 142–160. <https://doi.org/10.1111/J.1574-6941.2007.00375.X>

- Rinke, C., Rubino, F., Messer, L. F., Youssef, N., Parks, D. H., Chuvochina, M., Brown, M., Jeffries, T., Tyson, G. W., Seymour, J. R., & Hugenholtz, P. (2019). A phylogenomic and ecological analysis of the globally abundant Marine Group II archaea (Ca. Poseidoniales ord. nov.). *ISME Journal*, *13*(3), 663–675.  
<https://doi.org/10.1038/s41396-018-0282-y>
- R Core Team (2021). R: A language and environment for statistical computing. R Foundation for Statistical Computing, Vienna, Austria. URL <https://www.R-project.org/>.
- Santoro, A. E., & Casciotti, K. L. (2011). Enrichment and characterization of ammonia-oxidizing archaea from the open ocean: Phylogeny, physiology and stable isotope fractionation. *ISME Journal*, *5*(11), 1796–1808.  
<https://doi.org/10.1038/ISMEJ.2011.58>
- Santoro, A. E., Richter, R. A., & Dupont, C. L. (2019). Planktonic Marine Archaea. *Https://Doi.Org/10.1146/Annurev-Marine-121916-063141*, *11*, 131–158.  
<https://doi.org/10.1146/ANNUREV-MARINE-121916-063141>
- Sakai, S., Takaki, Y., Shimamura, S., Sekine, M., Tajima, T., Kosugi, H., Ichikawa, N., Tasumi, E., Hiraki, A. T., Shimizu, A., Kato, Y., Nishiko, R., Mori, K., Fujita, N., Imachi, H., & Takai, K. (2011). Genome Sequence of a Mesophilic Hydrogenotrophic Methanogen *Methanocella paludicola*, the First Cultivated Representative of the Order Methanocellales. *PLOS ONE*, *6*(7), e22898.  
<https://doi.org/10.1371/JOURNAL.PONE.0022898>
- Sakai, S., & Imachi, H. (2016). *Methanocella*. *Bergey's Manual of Systematics of Archaea and Bacteria*, 1–6. <https://doi.org/10.1002/9781118960608.GBM01366>
- Schloss, P. D., Westcott, S. L., Ryabin, T., Hall, J. R., Hartmann, M., Hollister, E. B., Lesniewski, R. A., Oakley, B. B., Parks, D. H., Robinson, C. J., Sahl, J. W., Stres,

- B., Thallinger, G. G., Van Horn, D. J., & Weber, C. F. (2009). Introducing mothur: Open-source, platform-independent, community-supported software for describing and comparing microbial communities. *Applied and Environmental Microbiology*, 75(23), 7537–7541. <https://doi.org/10.1128/AEM.01541-09>
- Schouten, S., Hopmans, E. C., Schefuß, E., & Sinninghe Damsté, J. S. (2002). Distributional variations in marine crenarchaeotal membrane lipids: a new tool for reconstructing ancient sea water temperatures? *Earth and Planetary Science Letters*, 204(1–2), 265–274. [https://doi.org/10.1016/S0012-821X\(02\)00979-2](https://doi.org/10.1016/S0012-821X(02)00979-2)
- Schouten, S., van der Meer, M. T. J., Hopmans, E. C., & Sinninghe Damsté, J. S. (2008). Comment on “Lipids of marine Archaea: Patterns and provenance in the water column and sediments” by Turich et al. (2007). In *Geochimica et Cosmochimica Acta* (Vol. 72, Issue 21, pp. 5342–5346). Elsevier Ltd. <https://doi.org/10.1016/j.gca.2008.03.028>
- Schouten, S., Villanueva, L., Hopmans, E. C., van der Meer, M. T. J., & Sinninghe Damsté, J. S. (2014). Are Marine Group II Euryarchaeota significant contributors to tetraether lipids in the ocean? *Proceedings of the National Academy of Sciences of the United States of America*, 111(41), E4285. <https://doi.org/10.1073/pnas.1416176111>
- Seyler, L. M., McGuinness, L. R., Gilbert, J. A., Biddle, J. F., Gong, D., & Kerkhof, L. J. (2018). Discerning autotrophy, mixotrophy and heterotrophy in marine TACK archaea from the North Atlantic. *FEMS Microbiology Ecology*, 94(3), 14. <https://doi.org/10.1093/FEMSEC/FIY014>
- Sharp, J. H. (2002). Analytical Methods for Total DOM Pools. In D. A. Hansell & C. A. Carlson (Eds.), *Biogeochemistry of Marine Dissolved Organic Matter* (2nd ed., pp. 35–49). Academic Press.

- Shi, W., & Wang, M. (2010). Characterization of global ocean turbidity from Moderate Resolution Imaging Spectroradiometer ocean color observations. *Journal of Geophysical Research: Oceans*, 115(C11), 11022. <https://doi.org/10.1029/2010JC006160>
- Shlimon, A. G., Friedrich, M. W., Niemann, H., Ramsing, N. B., & Finster, K. (2004). *Methanobacterium aarhusense* sp. nov., a novel methanogen isolated from a marine sediment (Aarhus Bay, Denmark). *International Journal of Systematic and Evolutionary Microbiology*, 54(3), 759–763. <https://doi.org/10.1099/IJS.0.02994-0/CITE/REFWORKS>
- Simon, M., Grossart, H. P., Schweitzer, B., & Ploug, H. (2002). Microbial ecology of organic aggregates in aquatic ecosystems. *Aquatic Microbial Ecology*, 28(2), 175–211. <https://doi.org/10.3354/AME028175>
- Smith, M. W., Allen, L. Z., Allen, A. E., Herfort, L., & Simon, H. M. (2013). Contrasting genomic properties of free-living and particle-attached microbial assemblages within a coastal ecosystem. *Frontiers in Microbiology*, 4(MAY), 120. <https://doi.org/10.3389/FMICB.2013.00120/BIBTEX>
- Sollai, M., Villanueva, L., Hopmans, E. C., Reichart, G. J., & Sinninghe Damsté, J. S. (2019). A combined lipidomic and 16S rRNA gene amplicon sequencing approach reveals archaeal sources of intact polar lipids in the stratified Black Sea water column. *Geobiology*, 17(1), 91–109. <https://doi.org/10.1111/GBI.12316>
- Sowers, K. R., & Gunsalus, R. P. (1988). Adaptation for growth at various saline concentrations by the archaeobacterium *Methanosarcina thermophila*. *Journal of Bacteriology*, 170(2), 998–1002. <https://doi.org/10.1128/JB.170.2.998-1002.1988>

- Strom, S. L. (2008). Microbial ecology of ocean biogeochemistry: A community perspective. *Science*, 320(5879), 1043–1045.  
<https://doi.org/10.1126/SCIENCE.1153527>
- Sturt, H. F., Summons, R. E., Smith, K., Elvert, M., & Hinrichs, K.-U. (2004). Intact polar membrane lipids in prokaryotes and sediments deciphered by high-performance liquid chromatography/electrospray ionization multistage mass spectrometry—new biomarkers for biogeochemistry and microbial ecology. *Rapid Communications in Mass Spectrometry*, 18(6), 617–628.  
<https://doi.org/10.1002/rcm.1378>
- Swan, B. K., Ehrhardt, C. J., Reifel, K. M., Moreno, L. I., & Valentine, D. L. (2010). Archaeal and bacterial communities respond differently to environmental gradients in anoxic sediments of a California hypersaline lake, the Salton Sea. *Applied and Environmental Microbiology*, 76(3), 757–768. <https://doi.org/10.1128/AEM.02409-09>
- Tee, H. S., Waite, D., Lear, G., & Handley, K. M. (2021). Microbial river-to-sea continuum: gradients in benthic and planktonic diversity, osmoregulation and nutrient cycling. *Microbiome* 2021 9:1, 9(1), 1–18. <https://doi.org/10.1186/S40168-021-01145-3>
- Teira, E., van Aken, H., Veth, C., & Herndl, G. J. (2006). Archaeal uptake of enantiomeric amino acids in the meso- and bathypelagic waters of the North Atlantic. *Limnology and Oceanography*, 51(1), 60–69.  
<https://doi.org/10.4319/lo.2006.51.1.0060>
- Turich, C., Freeman, K. H., Bruns, M. A., Conte, M., Jones, A. D., & Wakeham, S. G. (2007). Lipids of marine Archaea: Patterns and provenance in the water-column and sediments. *Geochimica et Cosmochimica Acta*, 71(13), 3272–3291.  
<https://doi.org/10.1016/j.gca.2007.04.013>

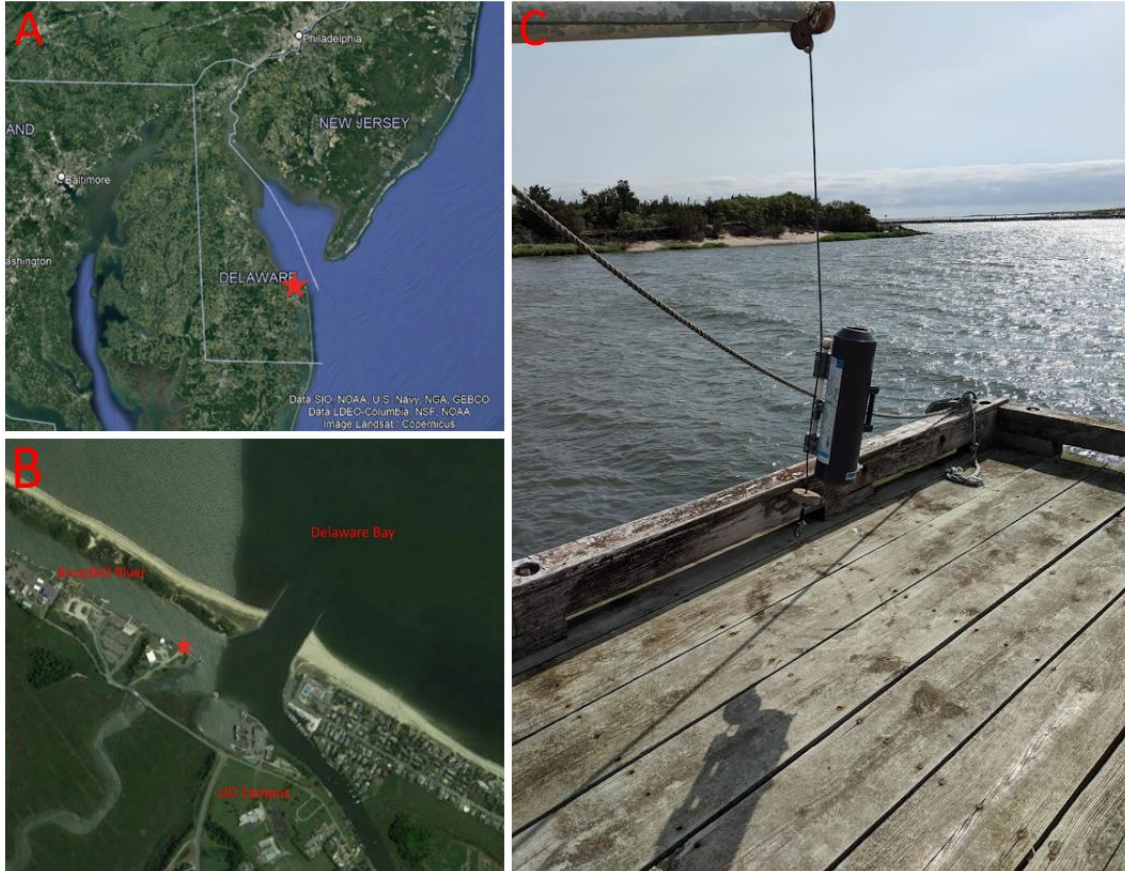
- Turich, C., Freeman, K. H., Jones, A. D., Bruns, M. A., Conte, M., & Wakeham, S. G. (2008). Reply to the Comment by S. Schouten, M. van der Meer, E. Hopmans, and J.S. Sinninghe Damsté on “Lipids of marine Archaea: Patterns and provenance in the water column.” In *Geochimica et Cosmochimica Acta* (Vol. 72, Issue 21, pp. 5347–5349). Elsevier Ltd. <https://doi.org/10.1016/j.gca.2008.04.042>
- Vieira, R. P., Clementino, M. M., Cardoso, A. M., Oliveira, D. N., Albano, R. M., Gonzalez, A. M., Paranhos, R., & Martins, O. B. (2007). Archaeal communities in a tropical estuarine ecosystem: Guanabara Bay, Brazil. *Microbial Ecology*, 54(3), 460–468. <https://doi.org/10.1007/S00248-007-9261-Y/FIGURES/4>
- Voynova, Y. G., Oliver, M. J., & Sharp, J. H. (2013). Wind to zooplankton: Ecosystem-wide influence of seasonal wind-driven upwelling in and around the Delaware Bay. *Journal of Geophysical Research: Oceans*, 118(12), 6437–6450. <https://doi.org/10.1002/2013JC008793>
- Wakeham, S. G., Hopmans, E. C., Schouten, S., & Sinninghe Damsté, J. S. (2004). Archaeal lipids and anaerobic oxidation of methane in euxinic water columns: a comparative study of the Black Sea and Cariaco Basin. *Chemical Geology*, 205(3–4), 427–442. <https://doi.org/10.1016/J.CHEMGEO.2003.12.024>
- Walker, C. B., de la Torre, J. R., Klotz, M. G., Urakawa, H., Pinel, N., Arp, D. J., Brochier-Armanet, C., Chain, P. S. G., Chan, P. P., Gollabgir, A., Hemp, J., Hügler, M., Karr, E. A., Könneke, M., Shin, M., Lawton, T. J., Lowe, T., Martens-Habbena, W., Sayavedra-Soto, L. A., ... Stahl, D. A. (2010). Nitrosopumilus maritimus genome reveals unique mechanisms for nitrification and autotrophy in globally distributed marine crenarchaea. *Proceedings of the National Academy of Sciences of the United States of America*, 107(19), 8818–8823. <https://doi.org/10.1073/pnas.0913533107>

- Wheeler, D. L., Barrett, T., Benson, D. A., Bryant, S. H., Canese, K., Chetvermin, V., Church, D. M., DiCuccio, M., Edgar, R., Federhen, S., Geer, L. Y., Kapustin, Y., Khovayko, O., Landsman, D., Lipman, D. J., Madden, T. L., Maglott, D. R., Ostell, J., Miller, V., ... Yaschenko, E. (2007). Database resources of the National Center for Biotechnology Information. *Nucleic Acids Research*, *35*(suppl\_1), D5–D12. <https://doi.org/10.1093/NAR/GKL1031>
- Wickham, H. (2009). *ggplot2: Elegant Graphics for Data Analysis*. In *ggplot2*. Springer New York. <https://doi.org/10.1007/978-0-387-98141-3>
- Wickham, H., Averick, M., Bryan, J., Chang, W., D'Almeida, L., McGowan, A., François, R., Grolemund, G., Hayes, A., Henry, L., Hester, J., Kuhn, M., Lin Pedersen, T., Miller, E., Bache, S. M., Müller, K., Ooms, J., Robinson, D., Seidel, D. P., ... Yutani, H. (2019). Welcome to the Tidyverse. *Journal of Open Source Software*, *4*(43), 1686. <https://doi.org/10.21105/JOSS.01686>
- Wuchter, C., Schouten, S., Wakeham, S. G., & Sinninghe Damsté, J. S. (2005). Temporal and spatial variation in tetraether membrane lipids of marine Crenarchaeota in particulate organic matter: Implications for TEX<sub>86</sub> paleothermometry. *Paleoceanography*, *20*(3), n/a-n/a. <https://doi.org/10.1029/2004PA001110>
- Wuchter, C. (2006). Seasonal dynamics of marine Archaea in coastal North Sea waters determined by different molecular approaches. In *Ecology and membrane lipid distribution of marine Crenarchaeota: Implication for the TEX<sub>86</sub> paleothermometry*. PhD thesis (pp. 41–64).
- Wuchter, C., Abbas, B., Coolen, M. J. L., Herfort, L., Van Bleijswijk, J., Timmers, P., Strous, M., Teira, E., Herndl, G. J., Middelburg, J. J., Schouten, S., & Damsté, J. S. S. (2006). Archaeal nitrification in the ocean. *Proceedings of the National Academy of Sciences of the United States of America*, *103*(33), 12317–12322. [https://doi.org/10.1073/PNAS.0600756103/SUPPL\\_FILE/00756FIG5.PDF](https://doi.org/10.1073/PNAS.0600756103/SUPPL_FILE/00756FIG5.PDF)

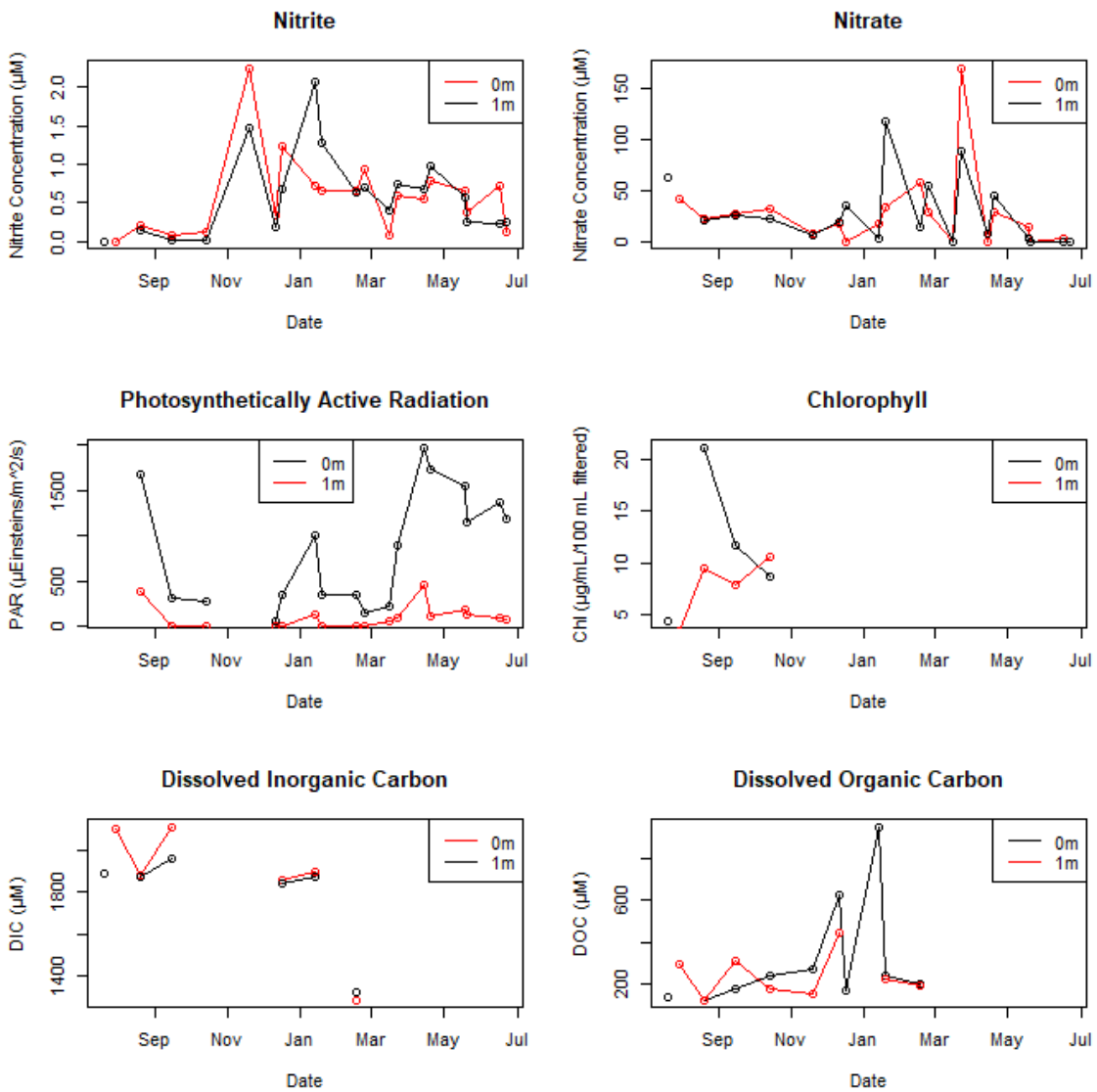
- Wuertz, Diethelm (2020). timeSeries: Financial Time Series Objects (Rmetrics). R package version 3062.100. <https://CRAN.R-project.org/package=timeSeries>
- Ye, W., Liu, X., Lin, S., Tan, J., Pan, J., Li, D., & Yang, H. (2009). The vertical distribution of bacterial and archaeal communities in the water and sediment of Lake Taihu. *FEMS Microbiology Ecology*, 70(2), 263–276. <https://doi.org/10.1111/J.1574-6941.2009.00761.X>
- Yoshimura, K. M., York, J., & Biddle, J. F. (2018). Impacts of salinity and oxygen on particle-associated microbial communities in the Broadkill River, Lewes DE. *Frontiers in Marine Science*, 5(MAR). <https://doi.org/10.3389/fmars.2018.00100>
- Zeikus, J. G., & Winfrey, M. R. (1976). Temperature limitation of methanogenesis in aquatic sediments. *Applied and Environmental Microbiology*, 31(1), 99. <https://doi.org/10.1128/AEM.31.1.99-107.1976>
- Zhuang, G. C., Peña-Montenegro, T. D., Montgomery, A., Montoya, J. P., & Joye, S. B. (2019). Significance of Acetate as a Microbial Carbon and Energy Source in the Water Column of Gulf of Mexico: Implications for Marine Carbon Cycling. *Global Biogeochemical Cycles*, 33(2), 223–235. <https://doi.org/10.1029/2018GB006129>

## Appendix A

### SUPPLEMENTAL FIGURES



**A.1.** Location of the study site and sampling setup. The red star in panel A indicates the location of zoomed-in panel B. The red star in panel B indicates the location of sampling. C shows an image of the sampling location and setup.

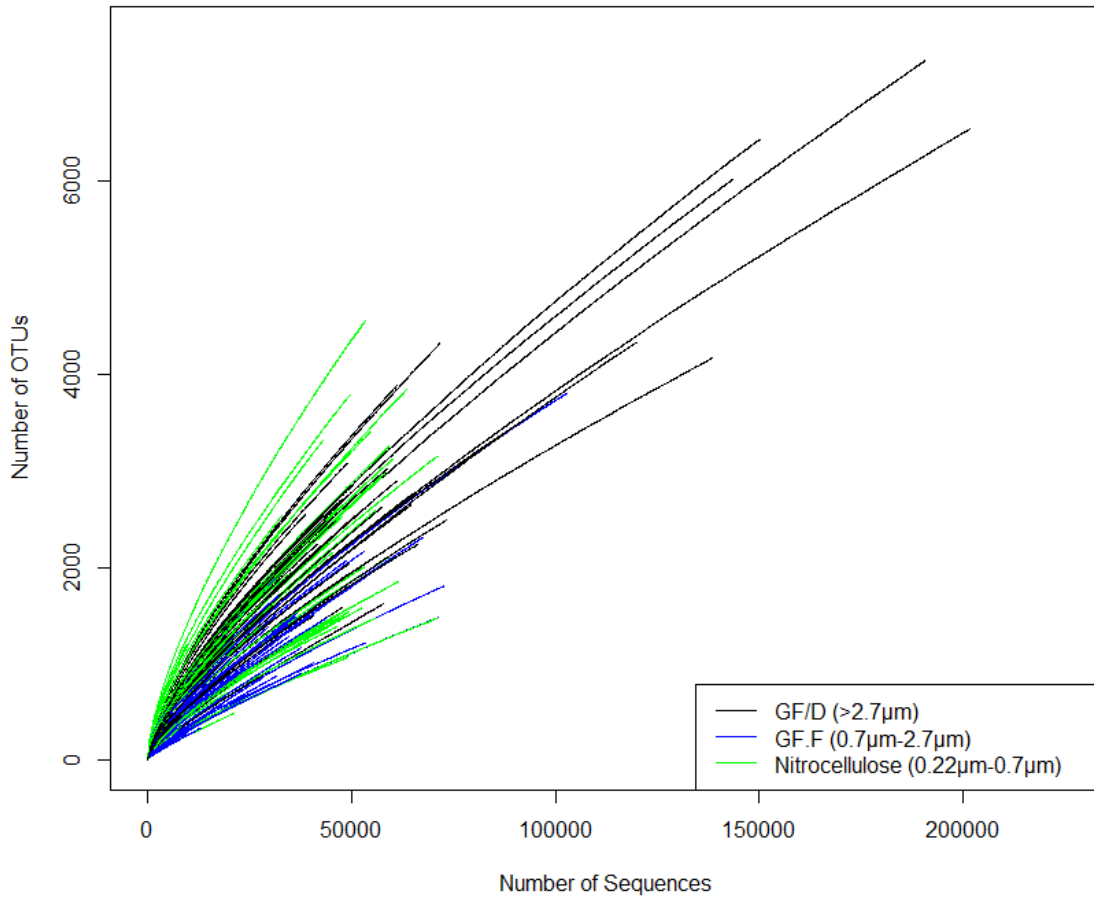


**A.2.** Plots of ancillary data over time at 0 m and 1 m: nitrite (A), nitrate (B), PAR (C), chlorophyll (D), DIC (E), and DOC (F).

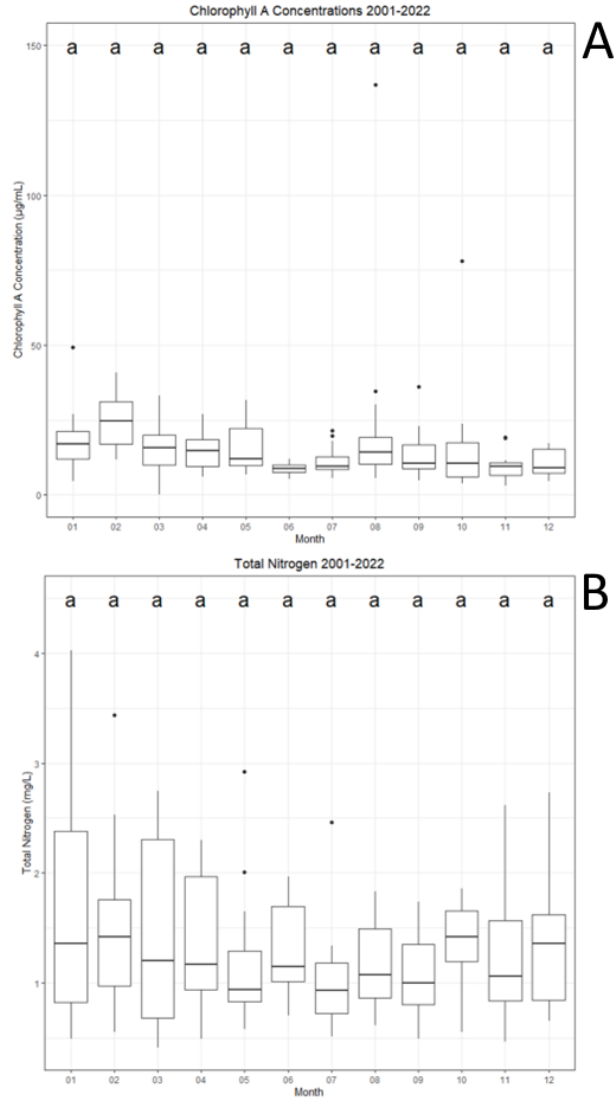


**A.3:** Annotated example of a successful gel – result of gel electrophoresis of PCR products using archaea-specific primers both with and without Illumina “wings”.

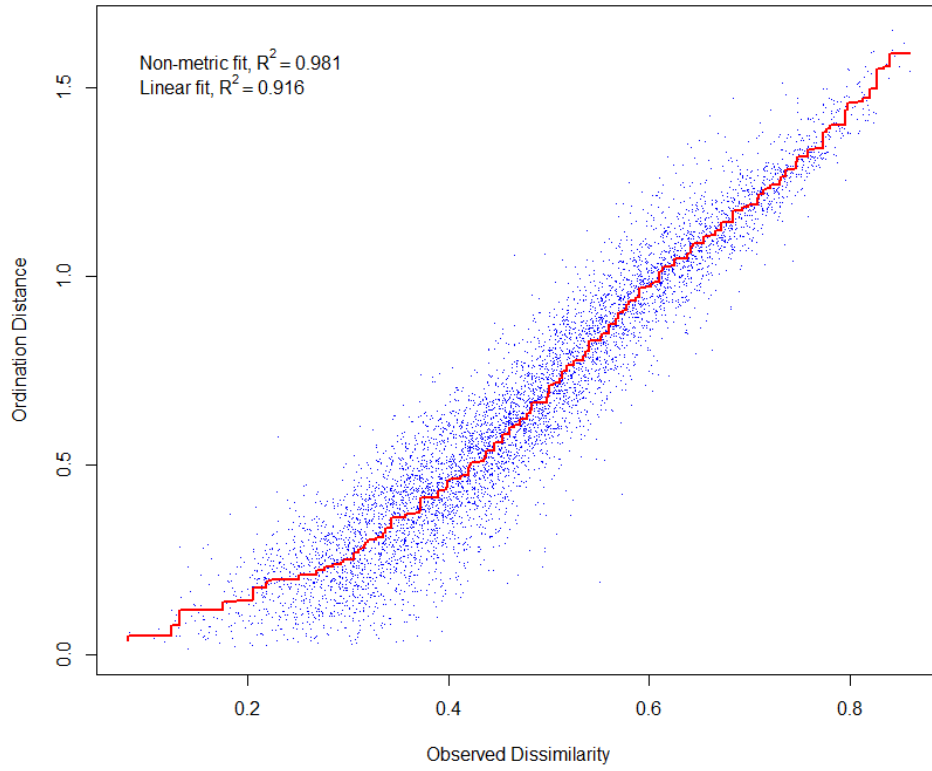
### Rarefaction Curves (Pre-Removal)



**A.4:** Rarefaction curves of all samples before removing low-abundance OTUs (those that appeared fewer than 10 times across all samples). Color-coded by pore size.

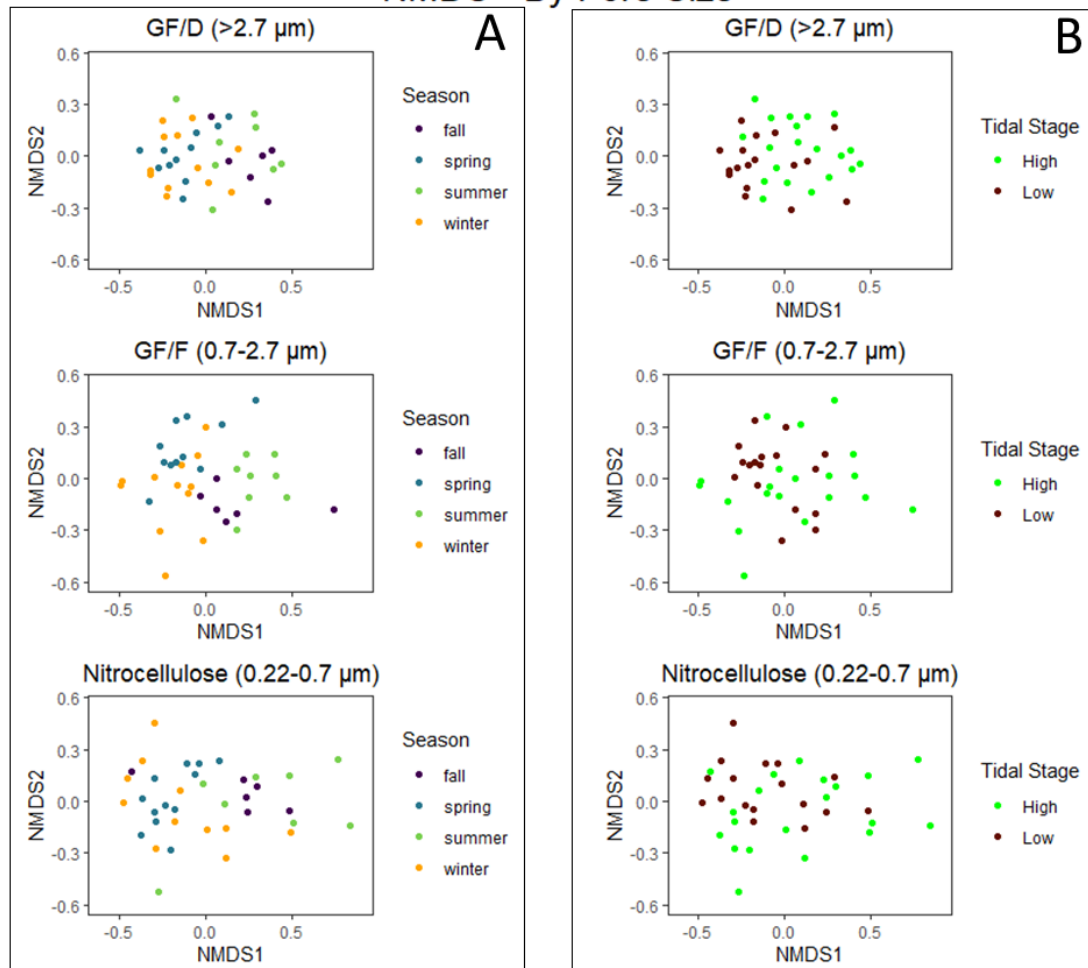


**A.5.** Box plot of monthly (A) chlorophyll a concentrations and (B) total nitrogen in the Broadkill river from 2001-2022. Lowercase letters at top represent groupings from Tukey’s HSD test; in this case, none are significantly different from any other. Data are from the Delaware Water Quality Portal (DNREC et al. 2022).

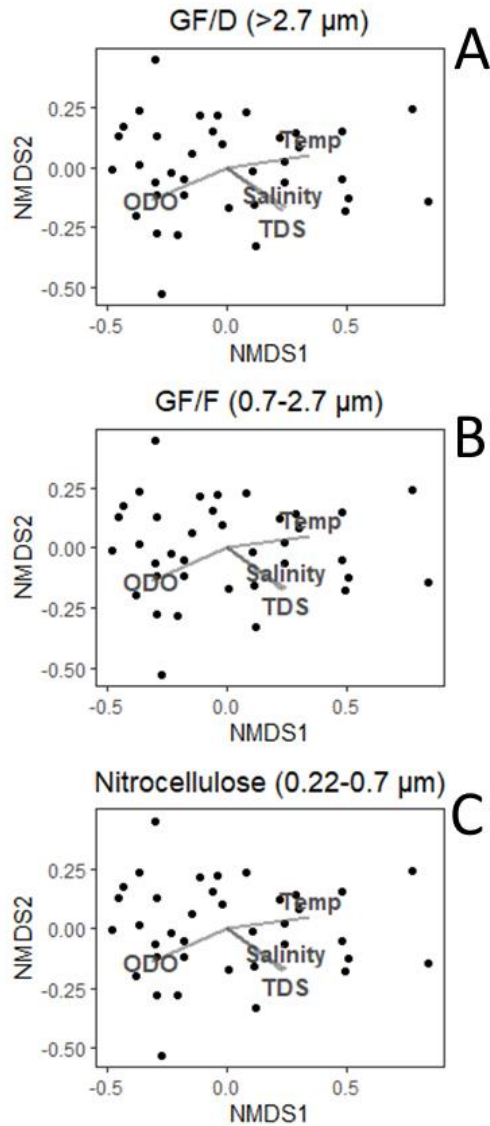


**A.6.** Stress plot for ordination of Bray-Curtis dissimilarity of all samples.

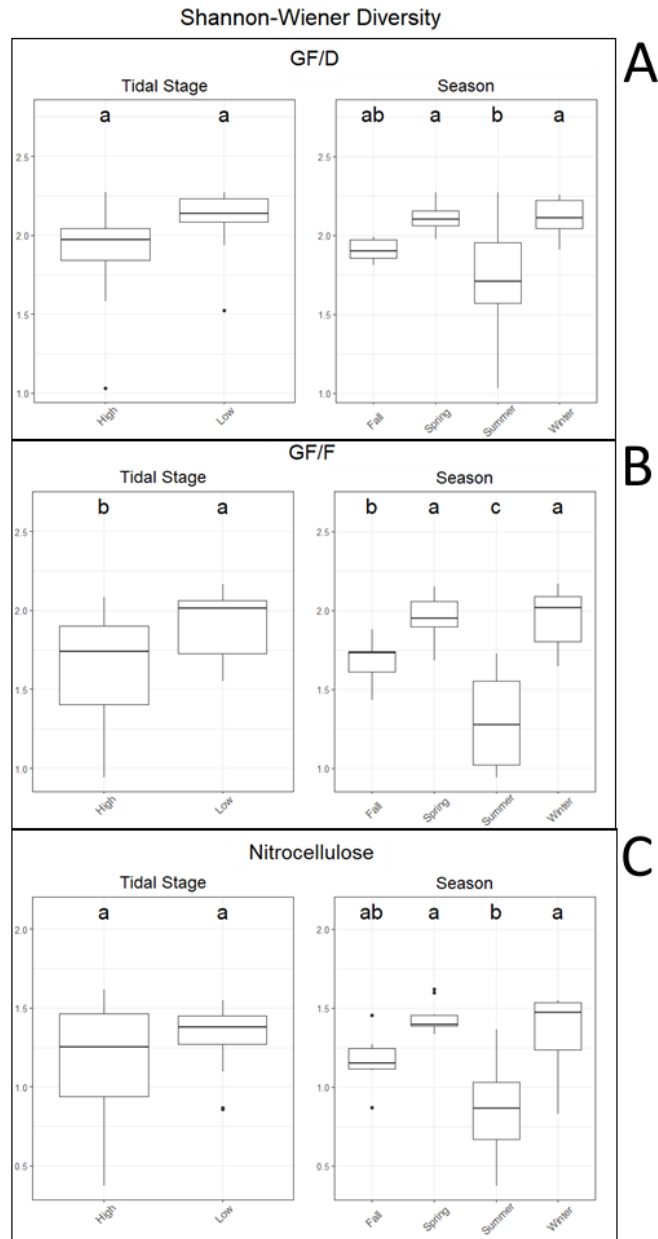
## NMDS - By Pore Size



**A.7:** NMDS plots created from separate ordinations for each pore size with colors denoting season (A) and tidal stage (B). Data are normalized by scaling with ranked sampling. Stress for the ordinations for GF/D, GF/F, and Nitrocellulose samples are 0.21, 0.21, and 0.19, respectively.



**A.8:** NMDS plots created from separate ordinations for the largest (A), middle (B), and smallest (C) pore sizes. Lines represent pseudo-axes constructed from environmental variables; the longer the arrow, the greater its predictive value of variation in the community. Stress for the ordinations for GF/D, GF/F, and Nitrocellulose samples are 0.21, 0.21, and 0.19, respectively.



**A.9:** Box plots of alpha diversity (Shannon-Wiener index) comparing samples grouped by category; done for the largest (A), middle (B), and smallest (C) pore sizes. Different lowercase letters represent groupings that are significantly different from each other according to Tukey's HSD test.

## Appendix B

### SUPPLEMENTAL TABLES

**B.1.** Nucleotide sequences and references for primers used. Illumina “wings” for the archaea-specific primers are in red.

<b>Primer Name</b>	<b>Primer Sequence</b>	<b>Target</b>	<b>Reference</b>
Illumina915F	5'- <b>ACA CTC TTT CCC TAC ACG CTC TTC</b> <b>CGA TCT</b> AGG AAT TGG CGG GGG AGC AC-3'	Archaeal 16S	Seyler et al. 2018
Illumina1059R	5'- <b>GTG ACT GGA GTT CAG ACG TGT</b> <b>GCT CTT CCG ATC TGC</b> CAT GCA CCW CCT CT-3'	Archaeal 16S	Seyler et al. 2018
B114F	5'-CGG CAA CGA GCG CAA CCC-3'	Bacterial 16S	Denman and McSweeney 2006
B1275R	5'-CCA TTG TAG CAC GTG TGT AGC C- 3'	Bacterial 16S	Denman and McSweeney 2006

**B.2.** Sampling dates and corresponding ancillary water chemistry data for nitrite, nitrate, photosynthetically active radiation (PAR), chlorophyll, dissolved inorganic carbon (DIC), and non-purgeable organic carbon (NPOC). For nitrite concentration and nitrate concentration, values are derived from a calibration curve and were sometimes negative; negative values have been converted to zeroes. Blank cells represent data that have not yet been generated.

Sampling date	Nitrite Concentration ( $\mu\text{M}$ )		Nitrate Concentration ( $\mu\text{M}$ )		PAR ( $\mu\text{Einsteins}/\text{m}^2/\text{s}$ )		Chlorophyll ( $\mu\text{g}/\text{L}$ )		DIC		NPOC ( $\mu\text{M}$ )	
	0m	1m	0m	1m	0m	1m	0m	1m	0m	1m	0m	1m
7/21/2020	0	N/A	62.58662	N/A	N/A	N/A	0.446875	N/A	1890.227	N/A	138.5	N/A
7/30/2020	N/A	0	N/A	42.30686	N/A	N/A	N/A	0.351759	N/A	2102.286	N/A	291.21
8/20/2020	0.137104	0.212144	20.03549	21.6953	1686.249	395.6884	2.11	0.94125	1871.345	1882.672	124.45	119.29
9/15/2020	0.01829	0.068317	25.53831	27.10349	308.5744	6.97698	1.176923	0.795	1965.709	2115.527	177.1	314.13
10/14/2020	0.012037	0.112091	22.31416	32.3839	272.2242	8.120012	0.871053	1.056667			242.91	176.21
11/19/2020	1.465227	2.24837	5.877649	8.119218	N/A	N/A	3.86	0.937143			271.51	152.3
12/11/2020	0.192619	0.33173	18.83664	17.80387	69.00934	0.776274	2.423529	4.5			625.01	446.3
12/17/2020	0.687236	1.233375	34.77172	0	357.2569	0.144801	8.466667	2.066667	1839.656	1856.053	171.48	
1/13/2021	2.068041	0.728454	2.868813	18.02584	1013.943	137.3645	1.17	0.566429	1874.508	1898.276	951.52	
1/19/2021	1.279745	0.656322	117.2901	33.08404	357.8766	12.88289	1.277895	5.111111			242.23	221.22
2/17/2021	0.625409	0.666627	13.45433	57.6839	349.0471	0	3.395	3.124	1316.177	1282.171	198.67	193.88
2/23/2021	0.692388	0.944849	55.18337	29.08337	151.3852	6.323034	3.25	4.417778				
3/16/2021	0.403862	0.068965	0	0	221.7685	67.18149	1.353103	1.92381				
3/23/2021	0.733606	0.599648	88.13902	170.5589	902.791	94.92414	3.145455	1.226				
4/14/2021	0.682084	0.548125	7.82943	0	1976.542	469.0912	2.818182	0.787273				
4/20/2021	0.97061	0.785129	45.69353	28.6244	1730.897	108.5644	5.221053	1.94				
5/18/2021	0.568734	0.666627	2.855764	13.34436	1548.908	199.2539	5.377778	1.452				
5/20/2021	0.249294	0.367796	0	0	1151.699	130.5716	1.544	0.633766				
6/16/2021	0.218381	0.712997	0	2.711501	1373.89	94.92012	8.48	0.908				
6/22/2021	0.249294	0.12564	0	0	1184.969	88.07035	2.847059	1.48				

**B.3.** Results of linear regressions comparing relative abundance of methanogens vs. MGI and MGII, relative abundance of Methanobacteria vs. Methanocellia, and the sum of the relative abundance of the four major methanogen classes vs. temperature. Orange cells indicate a significant negative correlation; yellow cells indicate a significant positive correlation.

Methanogen Class	Stat	MGI				MGII				MGI + MGII			
		GF/D		GF/F		GF/D		GF/F		GF/D		GF/F	
		0m	1m	0m	1m	0m	1m	0m	1m	0m	1m	0m	1m
Methanosarcinia	p-val	0.362199	0.0736	0.19727	0.333	2.54E-05	0.000224	0.1696	0.12179	1.51E-05	4.52E-05	0.06385	0.06489
	R <sup>2</sup>	0.04905	0.1864	0.1016	0.05524	0.6575	0.5837	0.1145	0.135	0.6773	0.6569	0.1985	0.1864
Methanobacteria	p-val	0.0247	0.034514	0.1655	0.29583	0.00197	0.00145	0.00245	0.000601	8.47E-05	0.000174	0.000541	0.000334
	R <sup>2</sup>	0.2632	0.2502	0.1166	0.06405	0.4398	0.4785	0.4461	0.5093	0.6069	0.596	0.5371	0.5407
Methanocellia	p-val	0.023967	0.0119	0.11509	0.143991	0.0106	0.0033	0.00213	0.00163	0.000962	0.000219	0.000249	0.00023
	R <sup>2</sup>	0.2665	0.3345	0.1479	0.1213	0.3267	0.4265	0.4551	0.4514	0.4827	0.5847	0.5783	0.5598
Methanomicrobia	p-val	0.09	0.0273	0.150742	0.203884	3.55E-06	1.01E-05	0.00541	0.00648	2.88E-08	1.51E-07	0.00111	0.00184
	R <sup>2</sup>	0.1598	0.2693	0.1246	0.09314	0.7269	0.7144	0.3924	0.3614	0.8438	0.8297	0.4956	0.4438
Methanogen Class	Stat	Methanocellia				Methanogen Class	Stat	Vs. Temperature					
		GF/D		GF/F				GF/D		GF/F			
		0m	1m	0m	1m			0m	1m	0m	1m		
Methanobacteria	p-val	5.35E-05	0.000243	0.00154	0.019	All Methanogens	p-val	0.00269	0.00269	0.00628	0.0081		
	R <sup>2</sup>	0.627	0.5794	0.4757	0.2832	Methanogens	R <sup>2</sup>	0.42	0.4401	0.3818	0.3458		

**B.4.** ANOSIM results for samples separated by pore size. Yellow cells indicate a significant (<0.05) p-value. “Yearsplit” indicates Dec-May vs. Jun-Nov.

	GF/D			GF/F			Nitrocellulose		
	Tide	Season	Yearsplit	Tide	Season	Yearsplit	Tide	Season	Yearsplit
<b>ANOSIM statistic R</b>	0.1509	0.4782	0.6931	0.1632	0.4601	0.5437	0.08155	0.376	0.4715
<b>Significance</b>	0.0077	1.00E-04	1.00E-04	0.0055	1.00E-04	1.00E-04	0.0579	1.00E-04	1.00E-04

**B.5.** Results of Mantel test evaluating relationship between Euclidean distance matrices constructed from environmental variables and a Bray-Curtis dissimilarity matrix of samples; done separately for each pore size. Highlighted cells indicate significant p-values.

	GF/D		GF/F		Nitrocellulose	
	Mantel statistic r	Significance	Mantel statistic r	Significance	Mantel statistic r	Significance
<b>Salinity</b>	0.1543	0.022	0.1952	0.0019	0.1919	0.0015
<b>TDS</b>	0.1343	0.0406	0.192	0.0025	0.1967	0.0019
<b>ODO</b>	0.277	1.00E-04	0.1095	0.0354	0.226	5.00E-04
<b>Temp</b>	0.407	1.00E-04	0.2559	1.00E-04	0.3144	1.00E-04